X-RAY DIFFRACTION AND OPTICAL REFRACTION OF WATER AND ELECTROLYTE SOLUTIONS

J.HEEMSKERK

X-RAY DIFFRACTION AND OPTICAL REFRACTION OF WATER AND ELECTROLYTE SOLUTIONS

X-RAY DIFFRACTION AND OPTICAL REFRACTION OF WATER AND ELECTROLYTE SOLUTIONS

PROEFSCHRIFT

TER VERKRIJGING VAN DE GRAAD VAN DOCTOR IN DE WIS- EN NATUURKUNDE AAN DE RIJKSUNIVERSITEIT TE LEIDEN, OP GEZAG VAN DE RECTOR MAGNIFICUS MR. J.E. JONKERS, HOOGLERAAR IN DE FACULTEIT DER RECHTSGELEERDHEID, TEGEN DE BEDENKINGEN VAN DE FACULTEIT DER WIS- EN NATUURKUNDE TE VERDEDIGEN OP DONDERDAG 17 DECEMBER 1959 TE 15 UUR

DOOR

JAN HEEMSKERK

GEBOREN TE 'S-GRAVENHAGE IN 1931

1959
BRONDER OFFSET ROTTERDAM

PROMOTOR: PROF. DR C.J.F. BÖTTCHER

Aan mijn ouders

Aan Janny

CONTENTS

INTRODUCTION

The purpose of the present investigations was to gain a better insight into three problems in the field of electrolyte solutions; these problems concern the "structure" of water, the hydration of ions and the interpretation of optical refraction measurements on electrolyte solutions.

One of the most promising techniques for this purpose, apart from the measurements of the optical refraction, seemed to be the application of X-ray diffraction methods. These are much more often applied to crystalline matter than to liquids since crystals are characterized by a regular arrangement of the constituent atoms, whereas such a regular arrangement is lacking in liquids. However, a certain regularity is also found in liquids owing to the impossibility of interpenetration of the atoms and to the fact that certain configurations of atoms with respect to their neighbours are more probable than others.

It is, in principle, possible to obtain from X-ray diffraction measurements information about the distances between the atoms and about the frequency with which these distances occur. In this thesis an attempt has been made to interpret X-ray diffraction measurements on liquids in terms of these two quantities. For this purpose it was necessary to consider in some detail the theory on which the interpretation of the measurements is based.

Several attempts have been made to describe the "structure" of water in terms of a quasi-crystalline model. The most important of the proposed models are the widely accepted tetrahedral model (Bernal and Fowler [1]) and the octahedral model (van Panthaleon van Eck, Mendel and Boog [2] ; van Panthaleon van Eck, Mendel and Fahrenfort [3]). An experimental basis for the tetrahedral arrangement was provided by the X-ray diffraction measurements of Morgan and Warren [4]. The results of more recent work on the X-ray diffraction of water [2,3], however, are in favour of an octahedral arrangement. One of the aims of our X-ray diffraction measurements on water at various temperatures was to examine whether a detailed analysis of the results makes it possible to decide on a model for the "structure" of water.

As it possible to obtain from X-ray diffraction measurements information about the frequency with which interatomic distances occur, this technique should, if used on concentrated electrolyte solutions,

in principle provide a method for the determination of hydration numbers of ions in solution. The hydration numbers of ions obtained from other experimental methods vary widely. This is mainly due to the fact that with most methods no sharp distinction can be made between primary and secondary hydration. In this thesis it is attempted to derive from X-ray diffraction measurements on KOH solutions at different concentrations a hydration number for the potassium ion. KOH was chosen because the OH^--ion is comparable in size and scattering power to the water molecule.

The results of the optical refraction measurements will be interpreted in terms of the Onsager-Böttcher theory [5]. This theory provides a method for the calculation of the polarizabilities and the radii of ions from the refractive indices and the densities of electrolyte solutions. An important quantity to be used in these calculations is the radius of the water molecule. It is not possible to calculate this radius from measurements of the optical refraction of water as in this case deviations from the Onsager-Böttcher theory occur. In this thesis, these deviations are attributed to the "structure" of water. The radius of the water molecule used until now for the calculation of the polarizabilities and the radii of ions was mainly based upon its value in the solid state. The value for the radius of the water molecule used in this thesis is based upon the X-ray diffraction measurements and upon the measurements of the optical refraction of water carried out by Tilton and Taylor [6].

Optical refraction measurements on electrolyte solutions were carried out in order to calculate the polarizabilities and the radii of a number of ions. Apart from this, it was decided to investigate whether the Onsager-Böttcher theory provides a basis for the study of the formation of complexes in solution.

A discussion of the theory on which the interpretation of the X-ray diffraction measurements is based is given in chapter I. Special attention is paid to the problem of the conversion of the observed intensities into absolute values.

The first part of chapter II describes the experimental technique of the X-ray diffraction measurements. Results are given for the X-ray diffraction of vitreous SiO_2; this example was chosen in order to test the experimental and the calculating technique. The results and the interpretation of the X-ray diffraction measurements on water and KOH solutions are given in the second part of this chapter.

Chapter III deals with the theory of the optical refraction of electrolyte solutions. Arguments are put forward for the introduction of the radius of the water molecule used in this thesis for the calculation of the polarizabilities and the radii of ions from optical

refraction measurements.

After a description of the experimental technique, the results of the measurements of the optical refraction of sodium nitrate, potassium nitrate and silver nitrate solutions and of solutions of potassium iodide + mercuric iodide in water are discussed in chapter IV.

CHAPTER I

X-RAY DIFFRACTION OF LIQUIDS

I.1. The distribution functions

This section deals with the basic concepts of the X-ray diffraction of liquids [7,8,9]. A derivation will be given of the fundamental equations on which the interpretation of the X-ray diffraction measurements described in chapter II is based.

We shall consider a medium with a mean electron density ρ_0, where the electron densities in the volume-elements dV_1 and dV_2, determined by the position vectors $\vec{p}$ and $\vec{p} + \vec{r}$, are given by $\rho(\vec{p})$ and $\rho(\vec{p} + \vec{r})$. Let $\vec{1}_0$ be the unit vector in the direction of the primary beam, $\vec{1}$ that in the direction of the scattered beam and λ the wave-length of the X-rays (fig.I.1).

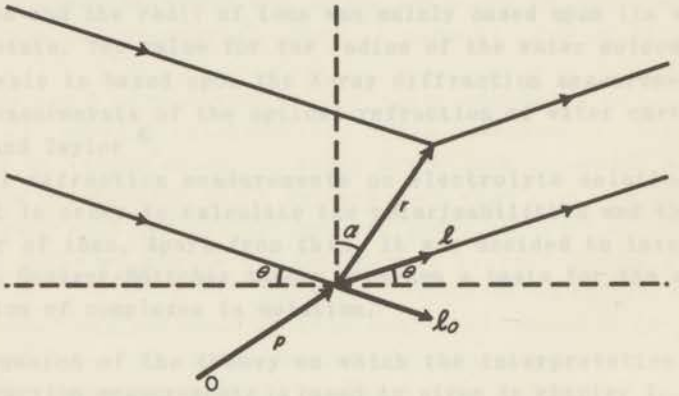

Figure I.1.

The path difference between the waves scattered by the electrons in these two volume-elements is given by

$$d = \vec{r}.(\vec{1} - \vec{1}_0) = 2r\sin\theta\cos\alpha \qquad (I.1)$$

and the corresponding phase difference by

$$\phi = \frac{4\pi r\sin\theta\cos\alpha}{\lambda} = sr\cos\alpha, \qquad (I.2)$$

where $s = \frac{4\pi\sin\theta}{\lambda}$

The intensity * of the scattered beam is given by

$$I = \left\{\rho(\vec{p})\,dV_1\right\}^2 + \left\{\rho(\vec{p}+\vec{r})\,dV_2\right\}^2 + 2\rho(\vec{p})\,\rho(\vec{p}+\vec{r})\cos\phi\,dV_1 dV_2. \qquad .3)$$

This holds for one specified position of dV_2 on the surface of a sphere with radius $|\vec{r}|$ and centre at $\vec{p}$. By averaging over all positions of dV_2 on the surface of this sphere, assuming $\rho(\vec{p}+\vec{r})$ to depend on $|\vec{r}|$ but not on $\vec{r}$, the following expression is obtained:

$$\bar{I} = \left\{\rho(\vec{p})\,dV_1\right\}^2 + \left\{\rho(\vec{p}+\vec{r})\,dA\,dr\right\}^2 + 2\rho(\vec{p})\,\rho(\vec{p}+\vec{r})\,\frac{\sin sr}{sr}\,dV_1\,dA\,dr, \quad (I.4)$$

where dA = surface-element on the sphere.
In order to obtain the total intensity of the coherently scattered radiation of a sample of volume V, expression (I.4) has to be integrated over all possible values of r, combined with an integration over the surface of a sphere with radius r and over all possible positions of the volume-element dV_1:

$$I_{coh}(s) = \int_0^\infty \int_V \int_A \rho(\vec{p})\,\rho(\vec{p}+\vec{r})\,\frac{\sin sr}{sr}\,dA\,dV\,dr, \qquad (I.5)$$

$\int_A dA$ means the integration over the surface of a sphere with radius $|\vec{r}|$ and origin at $\vec{p}$ and $\int_V dV$ the integration over the volume V of the irradiated sample.

For a sample consisting of N atoms, numbered 1,2,..,i,..,N, expression (I.5) leads to:

$$I_{coh}(s) = \int_0^\infty \int_V \int_A \sum_i \rho_i(\vec{p}) \sum_i \rho_i(\vec{p}+\vec{r})\,\frac{\sin sr}{sr}\,dA\,dV\,dr, \qquad (I.6)$$

where $\rho_i(\vec{p})$ is the contribution from atom i to the electron density at the point $\vec{p}$.
By introducing a pair distribution function $\sigma(r)$ defined by

$$\sigma(r) \equiv \int_V \int_A \sum_i \rho_i(\vec{p}) \sum_i \rho_i(\vec{p}+\vec{r})\,dA\,dV, \qquad (I.7)$$

---

* the unit scattered amplitude is taken as the amplitude scattered by a single classical electron under the same conditions.

the expression for the intensity of the coherently scattered radiation becomes:

$$I_{coh}(s) = \int_0^\infty \sigma(r) \frac{\sin sr}{sr} dr \ . \qquad (I.8)$$

A part of $I_{coh}(s)$ arises from distances within the atoms; this coherent background scattering is given by:

$$I_B(s) = \int_0^\infty \int_V \int_A \sum_i \rho_i(\vec{p}) \rho_i(\vec{p} + \vec{r}) \frac{\sin sr}{sr} dA dV dr = \sum_i f_i^2(s) \ , \qquad (I.9)$$

where $f_i(s)$ is the atomic form factor of atom i.
If a pair distribution function $\sigma_{at}(r)$, involving only distances within the atoms, is introduced, expression (I.9) can be written as

$$I_B(s) = \int_0^\infty \sigma_{at}(r) \frac{\sin sr}{sr} dr \ . \qquad (I.10)$$

The remaining part of $I_{coh}(s)$, which is due to order phenomena in the sample, is given by

$$I_M(s) = I_{coh}(s) - I_B(s) = \int_0^\infty \int_V \int_A \sum_{i \neq j} \sum \rho_i(\vec{p}) \rho_j(\vec{p} + \vec{r}) \frac{\sin sr}{sr} dA dV dr. \qquad (I.11)$$

Here we introduce a pair distribution function $\sigma_M(r)$, involving only distances between the atoms:

$$\sigma_M(r) \equiv \int_V \int_A \sum_{i \neq j} \sum \rho_i(\vec{p}) \rho_j(\vec{p} + \vec{r}) dA dV \cdot \qquad (I.12)$$

The expression for $I_M(s)$ now becomes:

$$I_M(s) = \int_0^\infty \left\{ \sigma(r) - \sigma_{at}(r) \right\} \frac{\sin sr}{sr} dr = \int_0^\infty \sigma_M(r) \frac{\sin sr}{sr} dr. \qquad (I.13)$$

Application of Fourier's integral theorem to equation (I.13) leads to

$$\frac{\sigma_M(r)}{r} = \frac{2}{\pi} \int_0^\infty s I_M(s) \sin(sr) ds \ . \qquad (I.14)$$

Knowing $I_M(s)$ one can calculate the distribution function $\sigma_M(r)$.

$I_M(s)$ can be obtained from our X-ray diffraction measurements.

except for the zero (and very small) angle scattering $I_0(s)$:

$$I_M(s) = I_M^E(s) + I_0(s) \ , \tag{I.15}$$

where $I_M^E(s)$ is the part of $I_M(s)$ that can be determined experimentally, giving it the value zero in the region of the zero-angle scattering. Equation (I.14) can now be written as

$$\frac{\sigma_M(r)}{r} = \frac{2}{\pi} \int_0^\infty s I_0(s) \sin(sr) ds + \frac{2}{\pi} \int_0^\infty s I_M^E(s) \sin(sr) ds. \tag{I.16}$$

The zero-angle scattering is the scattering from the whole irradiated sample, acting as one particle with uniform mean electron density ρ_0:

$$I_0(s) = \int_0^\infty 4\pi r^2 \rho_0^2 V \frac{\sin sr}{sr} dr \ . \tag{I.17}$$

Application of Fourier's integral theorem to equation (I.17) and substitution of the result into equation (I.16) gives

$$\frac{\sigma_M(r)}{r} = 4\pi r \rho_0^2 V + \frac{2}{\pi} \int_0^\infty s I_M^E(s) \sin(sr) ds \ . \tag{I.18}$$

As $I_M^E(s)$ can be determined experimentally, it is possible to calculate the distribution function $\sigma_M(r)$ from this formula.

Equation (I.12) can be written in an alternative form by introducing the deviation of the electron density $\rho_i(\vec{p})$ from the mean electron density per atom:

$$\rho_i(\vec{p}) = \frac{\rho_0}{N} + \Delta\rho_i(\vec{p}) \tag{I.19}$$

and consequently:

$$\rho(\vec{p}) = \rho_0 + \Delta\rho(\vec{p}) = \rho_0 + \sum_i \Delta\rho_i(\vec{p}) \ . \tag{I.20}$$

Making use of the equations (I.19) and (I.20) we obtain from formula (I.12):

$$\sigma_M(r) = 4\pi r^2 \rho_0^2 V + \int_V \int_A \sum_{i \neq j} \sum \Delta\rho_i(\vec{p}) \Delta\rho_j(\vec{p} + \vec{r}) dA dV = 4\pi r^2 \rho_0^2 V + \Delta\sigma_M(r). \tag{I.21}$$

Comparison of formulae (I.18) and (I.21) leads to:

$$\frac{\Delta\sigma_M(r)}{r} = \frac{2}{\pi}\int_0^\infty sI_M^E(s)\sin(sr)ds = \frac{1}{r}\int_V\int_A\sum_{i\neq j}\sum\Delta\rho_i(\vec{p})\Delta\rho_j(\vec{p}+\vec{r})dAdV. \tag{I.22}$$

For r values equal to interatomic distances of frequent occurrence $\Delta\sigma_M(r)$ will show a maximum.

A method for the interpretation of X-ray diffraction measurements on liquids containing more than one kind of atoms, used throughout the literature, involves the introduction of a factor K_i, the effective number of electrons around atom i, defined by:

$$K_i = \frac{f_i(s)}{f_e(s)}\ , \tag{I.23}$$

where $f_e(s)$ is the average scattering factor per electron, given by:

$$f_e(s) = \frac{\sum_i f_i(s)}{\sum_i Z_i} \tag{I.24}$$

(Z_i = atomic number of atom i).

In this method K_i is assumed to be a constant but it is in fact a function of s and may therefore not be treated as a constant in the evaluation of the Fourier transform. A further disadvantage of this method is the use of "point" atoms instead of the atoms with their actual electron distribution as this is bound to give rise to spurious diffraction ripples in the transform. These show up in the first part of the distribution functions as can be seen for example from the work of Warren. Krutter and Morningstar [10], Brady and Krause [11] and Brady [12]. Therefore the results obtained from analysis of distribution functions calculated by this method must be considered with due reserve.

I.2. The scaling factor

The intensity of the radiation originating from the sample, $I_A(s)$ on an absolute scale, is built up of several parts:

$$I_A(s) = I_B(s) + I_M(s) + I_C(s) + I_{Fl}(s)\ , \tag{I.25}$$

$I_B(s)$ = coherent background scattering,
$I_M(s)$ = coherent scattering due to order phenomena,
$I_C(s)$ = incoherent background scattering (Compton radiation),

$I_{Fl}(s)$ = fluorescence radiation.

$I_{Fl}(s)$ can be eliminated experimentally by selective filtering, leading to:

$$I_M(s) = I_A(s) - [I_B(s) + I_C(s)] . \qquad (I.26)$$

$I_B(s)$ and $I_C(s)$ can be calculated on an absolute scale from the chemical composition of the sample. In order to calculate $I_M(s)$ from equation (I.25), $I_A(s)$ has therefore to be known on an absolute scale. The experimentally observed intensity originating from a sample containing N atoms equals $NI^E(s)$ which is related to $I_A(s)$ in the following way:

$$I_A(s) = \alpha NI^E(s) + I_0(s), \qquad (I.27)$$

where α is a factor which will bring the experimentally observed intensity to an absolute scale and where $I_0(s)$ is defined by (I.17).

In the present thesis, the method of Krogh-Moe [13] and Norman [14] has been followed for the determination of the scaling factor α. By applying this method, all the information obtainable from the X-ray diagram is used in the calculation of the scaling factor. Its basic principles are outlined in the following part of this section.

Substitution of equation (I.27) into (I.26) leads to

$$I_M(s) = \alpha NI^E(s) + I_0(s) - [I_B(s) + I_C(s)]. \qquad (I.28)$$

Multiplication of both sides with $s\sin(sr)$ and integration between the limits 0 and s, where s is the highest experimentally accessible value of s, gives

$$\int_0^s sI_M(s)\sin(sr)ds = \int_0^s \alpha NsI^E(s)\sin(sr)ds + \int_0^s sI_0(s)\sin(sr)ds - \int_0^s s[I_B(s) + I_C(s)]\sin(sr)ds . \qquad (I.29)$$

As $I_0(s)$ has a value different from zero over a very limited range of s-values only, the upper integration limit in the second term on the right-hand side of equation (I.29) can be replaced by infinity. Application of Fourier's integral theorem to equation (I.17) gives:

$$\int_0^s sI_0(s)\sin(sr)ds = \int_0^\infty sI_0(s)\sin(sr)ds = 2\pi^2 r\rho_0^2 V . \qquad (I.30)$$

Combining equations (I.29) and (I.30) and introducing the mole fractions of the atoms results, after rearrangement, in

$$\frac{1}{N}\int_0^s s^2 I_M(s)\,\frac{\sin sr}{sr}\,ds - 2\pi^2\,\frac{N}{V}\,\bar{z}^2 = \alpha\int_0^s s^2 I^E(s)\,\frac{\sin sr}{sr}\,ds - \int_0^s s^2 \sum_i m_i\,[f_i^2(s) + I_C^i(s)]\,\frac{\sin sr}{sr}\,ds\,, \quad (I.31)$$

m_i = mole fraction of atoms i,

$\bar{z}$ = $\sum_i m_i z_i$, with z_i = number of electrons of atom i,

$I_C^i(s)$ = incoherent scattering of atoms i.

The next step is to consider the limiting case for $r \to 0$. It can easily be seen from equation (I.11) that if there is no overlap of the electron shells of atoms i and j the first term on the left-hand side of equation (I.31) will be zero for $r \to 0$ and thus

$$-2\pi^2\,\frac{N}{V}\,\bar{z}^2 = \alpha\int_0^s s^2 I^E(s)\,ds - \int_0^s s^2 \sum_i m_i\,[f_i^2(s) + I_C^i(s)]\,ds\,. \quad (I.32)$$

The assumption that there is no overlap of the electron shells will be the better fulfilled the higher the value of the upper integration limit and therefore the usefulness of equation (I.32) for the calculation of the scaling factor depends upon the convergence of the difference between the two integrals on the right-hand side of this equation with increasing s. This point will be discussed in more detail in the following section.

I.3. Discussion

In using formula (I.32) for the calculation of the scaling factor, we have neglected the term

$$\frac{1}{N}\int_0^s s^2 I_M(s)\,ds\,.$$

This results in an error $\delta\alpha$ in α, given by

$$\delta\alpha = \frac{\frac{1}{N}\int_0^s s^2 I_M(s)\,ds}{\int_0^s s^2 I^E(s)\,ds} \qquad (I.33)$$

This error has been calculated for cellulose by Norman [14]. His results show (table I.1) that even in the case of such a regular arrangement $\delta\alpha$ can be neglected at the higher values of the upper integration limit.

Table I.1

$\delta\alpha$ for cellulose (Norman [14])

s	$\frac{\delta\alpha}{\alpha}$ 100 %
3	30
5	5
7	< 3

The applicability of formula (I.32) for the calculation of the scaling factor depends on the convergence of α with increasing upper integration limit. By way of example table I.2 gives the scaling factors, as a function of the upper integration limit, for the X-ray diffraction of water at 0^oC and of a KOH solution (concentration 5.0 mole/litre).

Table I.2

Convergence of the scaling factor

s	α (H_2O, 0^oC)	α (KOH, 5.0 mol/l)
2	1.48	1.85
4	1.68	1.66
6	1.70	1.67
8	1.69	1.68

It can be seen from these examples that there is a rapid convergence of α with increasing upper integration limit. The scaling factors adopted in these two cases were 1.69 and 1.68.

Another method for the conversion of the observed intensities into absolute values uses only a small part of the information obtainable from the X-ray diagram. For high enough values of s, $I_M(s)$ can be taken as zero. $I_B(s) + I_C(s)$ can be calculated as a function of s and this curve can be matched with the experimental $I^E(s)$ curve at the high values of s. A serious disadvantage of this commonly applied method is that the accuracy required for a reliable determination of α is difficult to obtain at the high values of s, making the final choice of α somewhat arbitrary.

CHAPTER II

RESULTS AND DISCUSSION OF X-RAY DIFFRACTION MEASUREMENTS

II.1. Experimental

The experimental technique used for the X-ray diffraction measurements has been described by van Panthaleon van Eck, Mendel and Boog [2] and therefore only a short description will be given here.

In all experiments Cu K_α-radiation was used and consequently the diffraction patterns were obtained up to $s = 8$. The X-ray beam was monochromatized by the (200) reflection of a flat LiF crystal. The diffraction patterns were recorded on a film (Kodak Definix) fitted in a cylindrical camera (radius 2.9 cm). The film was protected from light on the inner side by an aluminium foil (thickness 25 μ) which was sandwiched between two Kel-F foils, $(-C_2F_3Cl-)_n$, (thickness 200 μ each). These latter foils absorb the fluorescence radiation originating from the samples used in this investigation.

The scattering registered on the film should originate from the sample only. This was achieved by using a liquid jet (diameter about 0.04 cm) as a specimen. This liquid jet could be centered accurately along the axis of the camera. The liquid, circulating through a closed system, was kept at a constant temperature. To eliminate air scattering helium was pumped through the camera. Exposure times were in the range of 12-20 hours.

The values of the film blackenings were converted into intensities by a calibrated, automatic recording, microphotometer. The non-exposed part of the film was taken as zero level. From the photometer diagram, intensity readings were taken at intervals of $\Delta s = 1/8$; these intensities were corrected for absorption and polarization [15].

The Fourier transforms were evaluated on an electronic computer; an interval of $\Delta r = 0.0625$ Å was taken. The functions $f_i(s)$ and $I_C^i(s)$ were taken from the sources compiled in table II.1.

Table II.1

References for $f_i(s)$ and $I_C^i(s)$

	$f_i(s)$	$I_C^i(s)$
H	16	-
O	17	18
K^+	17	19
Si	20	15

The experimental results will be given in terms of the total distribution functions

$$D(r) = \frac{\pi}{2} \frac{\sigma_M(r)}{r} \qquad (II.1)$$

and in terms of the distribution functions

$$\Delta D(r) = \frac{\pi}{2} \frac{\Delta\sigma_M(r)}{r} \qquad (II.2)$$

representing the difference between the actual total distribution function and that corresponding to a uniform medium.

In order to test the experimental and the calculating techniques, X-ray diffraction measurements were made on vitreous SiO_2. This substance was chosen because the interatomic Si-O distance in the various modifications of quartz is accurately known and because it is also known that in SiO_2 each silicon atom is surrounded by four oxygen atoms.

The scattering curve shown in figure II.1 was obtained by using a cylindrical rod of vitreous SiO_2, diameter 0.048 cm, as a specimen.

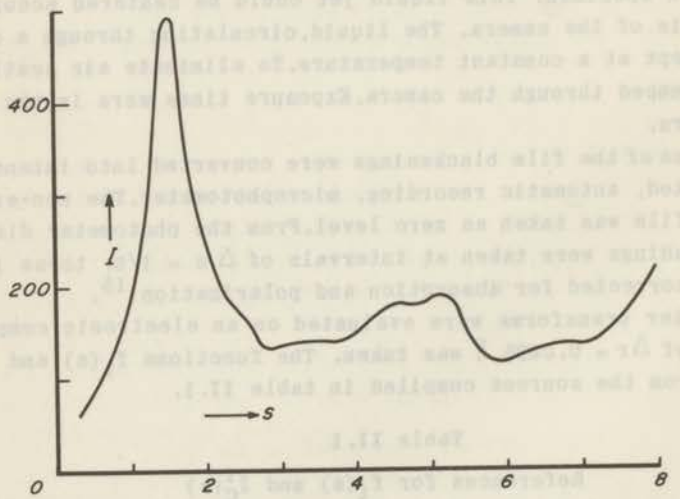

Figure II.1. Observed intensity for vitreous SiO_2 (uncorrected, arbitrary scale).

This scattering curve was corrected for absorption and polarization and from the resulting curve the distribution function for vitreous SiO_2 was calculated. This function is represented in figure II.2.

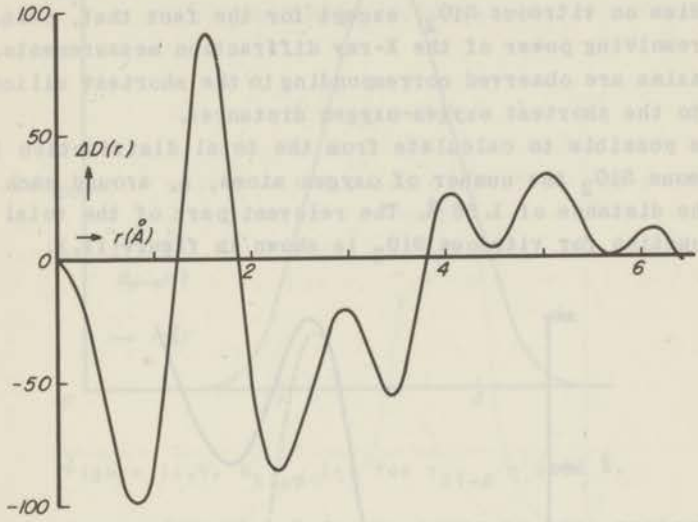

Figure II.2. Distribution function for vitreous SiO_2.

The first maximum in this curve, at 1.56 ± 0.06 Å, obviously gives the Si-O distance in vitreous SiO_2. We can now compare this interatomic distance with the Si-O distances given in the literature for quartz [21] and for vitreous SiO_2, the latter having been investigated by means of X-ray diffraction (Warren, Krutter and Morningstar [10]) and by means of neutron diffraction (Milligan, Levy and Peterson [22]).

Table II.2

Silicon-oxygen distances

	r_{Si-O} (Å)
low quartz [21]	1.61
low cristobalite [21]	1.58-1.69
vitreous SiO_2 [10]	1.62
vitreous SiO_2 [22]	1.58

It can be seen from table II.2 that our value of 1.56 Å for the Si-O distance is in good agreement with the values given in the literature. The positions of the remaining maxima in our distribution curve agree with those in the distribution curve obtained from neutron diffraction studies on vitreous SiO_2, except for the fact that, owing to the limited resolving power of the X-ray diffraction measurements, no separate maxima are observed corresponding to the shortest silicon-silicon and to the shortest oxygen-oxygen distances.

It is possible to calculate from the total distribution function for vitreous SiO_2 the number of oxygen atoms, n, around each silicon atom at the distance of 1.56 Å. The relevant part of the total distribution function for vitreous SiO_2 is shown in figure II.3.

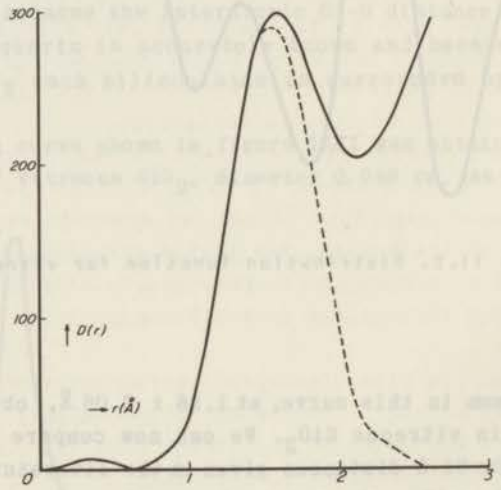

Figure II.3. Total distribution function for vitreous SiO_2.

The total distribution function of an oxygen atom and a silicon atom at a distance r' apart is given by:

$$D_{Si\text{-}O}(r) = \int_0^8 2f_O(s) f_{Si}(s) \frac{\sin sr'}{sr'} s \sin(sr) ds \,. \qquad (II.3)$$

This function, for r' = 1.56 Å, is shown in figure II.4.

In first approximation n can be calculated from the peak heights of the functions D(r) and $D_{Si\text{-}O}(r)$ at r = 1.56 Å:

$$m_{Si} n \, D_{Si\text{-}O}(r) = D(r) \quad \text{for } r = 1.56 \text{ Å}. \qquad (II.4)$$

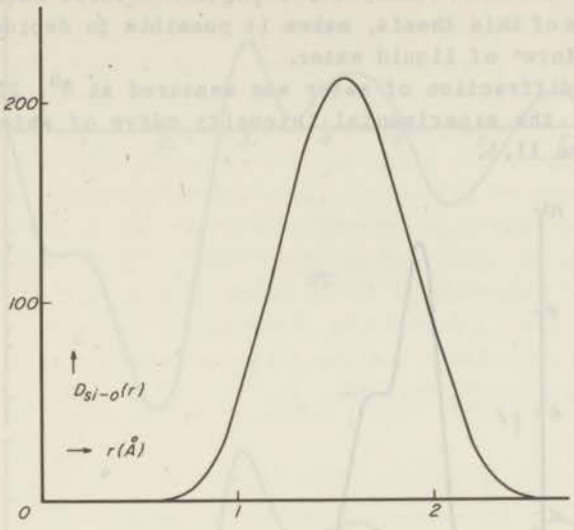

Figure II.4. $D_{Si-O}(r)$ for $r_{Si-O} = 1.56$ Å.

This results in a value of 4.2 for n; sence we have neglected the overlap due to other interatomic distances, the true value of n will be somewhat lower than 4.2. Another method for the calculation of n uses, instead of the peak heights, the areas under the curves D(r) and $D_{Si-O}(r)$. This calculation gives a value of 3.8 for n. However, due to the overlap it is not possible to determine the area under the curve in figure II.3 unambiguously. The values calculated for n are in fair agreement with the expected value of 4.0. This example shows that a reliable interpretation of the X-ray diffraction measurements in terms of interatomic distances and coordination numbers is possible.

II.2. X-ray diffraction of water *

Among earlier attempts to determine the "structure" of water is that of Morgan and Warren [4], who carried out X-ray diffraction measurements on water and interpreted their results in terms of a tetrahedral arrangement of the water molecules. More recent work on the X-ray diffraction of water by van Panthaleon van Eck, Mendel and Boog [2] and van Panthaleon van Eck, Mendel and Fahrenfort [3] has led to a model in which the water molecules are essentially sixfold coordinated. We car-

* The author's thanks are due to Miss P. J. M. A. Ekkers for her assistance in carrying out the measurements.

ried out X-ray diffraction measurements on water in order to investigate whether a detailed analysis, using the methods outlined in the preceding parts of this thesis, makes it possible to decide on a model for the "structure" of liquid water.

The X-ray diffraction of water was measured at 0^{o}, 25^{o} and 45^{o}C. As an example, the experimental intensity curve of water at 0^{o}C is shown in figure II.5.

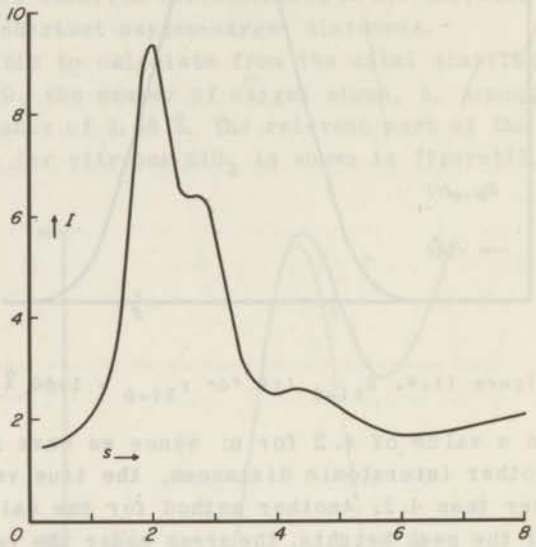

Figure II.5. Observed intensity for water at 0^{o}C (uncorrected, arbitrary scale).

The observed intensities were corrected for absorption and polarization and the distribution functions shown in figure II.6 were calculated. The main difference between these three curves is to be found in the third maximum; with rising temperature there is a decrease in the height of this maximum and it becomes less well defined.

The positions of the first three peaks are given in table II.3, together with an estimate of the accuracy with which these positions were determined.

Table II.3

Positions of the maxima in the distribution functions of water

t^{o}C	1st maximum (Å)	2nd maximum (Å)	3rd maximum (Å)
0	1.03 ± 0.15	3.00 ± 0.10	4.29 ± 0.15
25	0.81 ,,	2.97 ,,	4.38 ,,
45	0.88 ,,	3.06 ,,	4.26 ,,

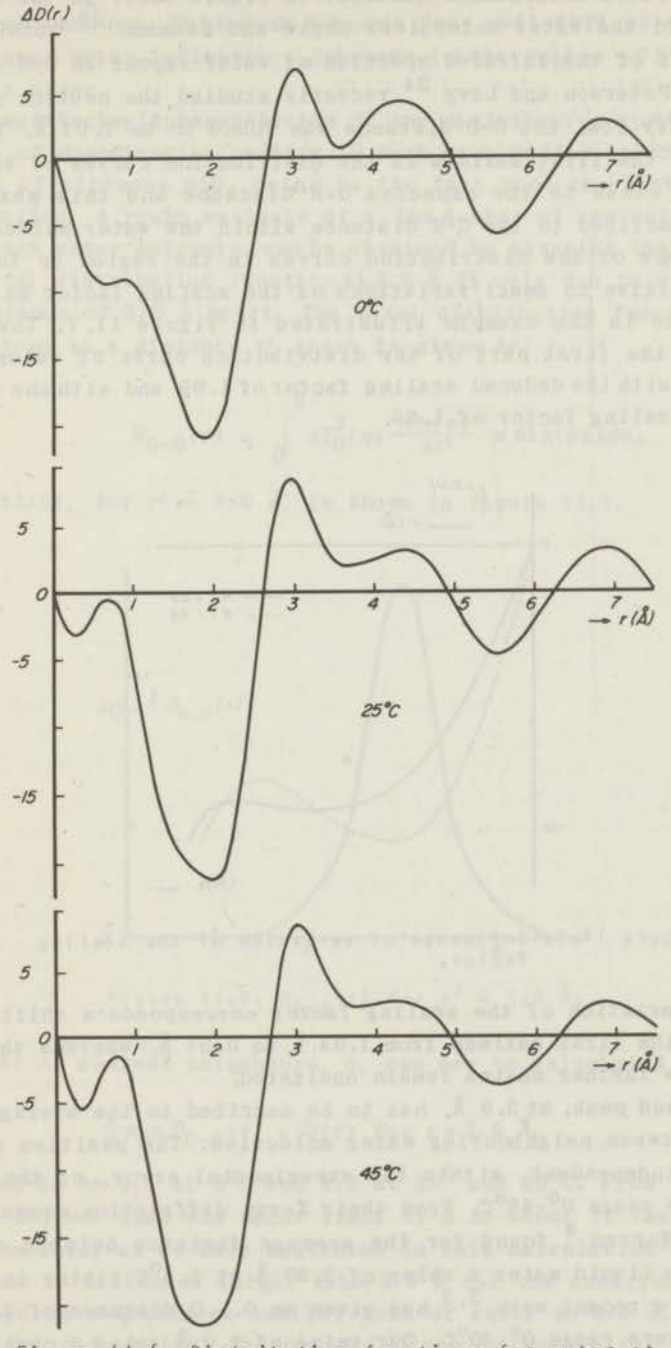

Figure II.6. Distribution functions for water at various temperatures.

The shortest interatomic distance in liquid water is the O-H distance within the water molecules. Mecke and Baumann [23] obtained from the analysis of the infrared spectrum of water vapour an O-H distance of 0.96 Å. Peterson and Levy [24] recently studied the neutron diffraction of heavy ice; the O-D distance was found to be 1.01 Å. The mean position of the first maximum in the distribution curves of water, at 0.91 Å, is close to the expected O-H distance and this maximum is therefore ascribed to the O-H distance within the water molecules.

The shape of the distribution curves in the region up to 1 Å is rather sensitive to small variations of the scaling factor as will be demonstrated in the example illustrated in figure II.7. The figure represents the first part of the distribution curve of water at 0°C calculated with the deduced scaling factor of 1.69 and with the slightly different scaling factor of 1.66.

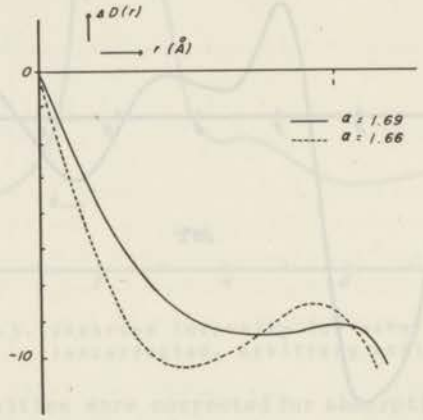

Figure II.7. Influence of variation of the scaling factor.

With this variation of the scaling factor corresponds a shift in the position of the first maximum from 1.03 Å to 0.97 Å, whereas the positions of the further maxima remain unaltered.

The second peak, at 3.0 Å, has to be ascribed to the average O...O distance between neighbouring water molecules. The position of this maximum is independent, within the experimental error, of the temperature in the range 0°-45°C. From their X-ray diffraction measurements Morgan and Warren [4] found for the average distance between closest neighbours in liquid water a value of 2.90 Å at 1.5°C rising to 3.05 Å at 83°C; more recent work [2,3] has given an O...O distance of 3.1 Å in the temperature range 0°-60°C. Our value of 3.0 Å takes a position in between the values quoted.

The third peak at about 4.3 Å is due to the distance between next-nearest neighbours. This peak becomes less well defined with rising temperature, which indicates a decrease in the degree of next-nearest neighbour order.

A quantitative interpretation of the distribution curves of water in terms of coordination numbers is much more difficult than it is in the case of vitreous SiO_2 owing to the fact that the peaks are less well resolved. A rough estimate of n, the number of nearest neighbours around each water molecule, can be obtained by assuming that the value of the total distribution function at 3.0 Å is only due to oxygen atoms at a distance of 3.0 Å apart. The total distribution function of two oxygen atoms at a distance r' apart is given by:

$$D_{O-O}(r) = \int_0^8 2f_O^2(s) \frac{\sin sr'}{sr'} s \sin(sr) ds. \qquad (II.5)$$

This function, for r' = 3.0 Å, is shown in figure II.8.

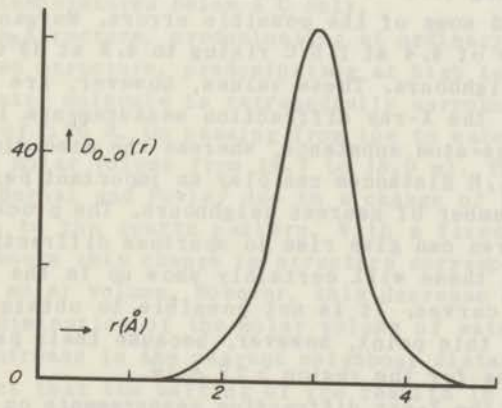

Figure II.8. $D_{O-O}(r)$ for r' = 3.0 Å.

The number of nearest neighbours, n, can now be calculated from:

$$\frac{1}{2} m_O n D_{O-O}(r) = D(r) \text{ for } r = 3.0 \text{ Å}. \qquad (II.6)$$

n is found to be 7.1 at 0°C and 7.2 at 25° and 45°C. From this calculation it follows that the upper limit of n is about 7. The true value of n will be lower as we have neglected in this calculation the overlap from peaks at distances larger than 3.0 Å and the contributions from oxygen-hydrogen distances smaller than or equal to 3.0 Å. To see to what extent this latter approximation can influence the calculated value of n, the calculation has been repeated assuming a maximum num-

ber of O...H distances at 3.0 Å (by placing the hydrogen atoms at the positions of the oxygen atoms).
In this case n follows from:

$$\frac{1}{2} m_O n D_{O-O}(r) + 2m_O n D_{O-H}(r) = D(r) \text{ for } r = 3.0 \text{ Å}, \quad (II.7)$$

where

$$D_{O-H}(r) = \int_0^8 2f_O(s) f_H(s) \frac{\sin sr'}{sr'} s \sin(sr) ds \text{ with } r' = 3.0 \text{ Å}. \quad (II.8)$$

The number of nearest neighbours is now calculated to be 5.1 at 0°C and 5.2 at 25° and 45°C. This calculation clearly demonstrates that the contributions from the O...H distances can play an important part in the calculation of n. In this connection it must be emphasized that Mendel [25] in deriving from his X-ray data a coordination number of 6 ± 0.5 underestimated some of the possible errors. Morgan and Warren [4] calculated a value of 4.4 at 1.5°C rising to 4.9 at 83°C for the number of nearest neighbours. These values, however, are based upon an interpretation of the X-ray diffraction measurements in which water is treated as a one-atom substance, whereas the preceding calculation has shown that O...H distances can play an important part in the calculation of the number of nearest neighbours. The procedure followed by Morgan and Warren can give rise to spurious diffraction ripples in the transform and these will certainly show up in the first part of the distribution curves. It is not possible to obtain any definite information about this point, however, because their paper gives the distribution curves for the region > 2 Å only.

The results of the X-ray diffraction measurements on water will be further discussed in the following section where we shall examine the various models proposed for the "structure" of water.

II.3. The "structure" of water

There have been made several attempts to explain the properties of water on the basis of a quasi-crystalline model. Bernal and Fowler [1] suggested a model in which the water molecules are tetrahedrally surrounded by four others, whereas van Panthaleon van Eck, Mendel and Boog [2] proposed an octahedral model in which the water molecules have a sixfold coordination. It will be examined in this section which of these two models gives the best agreement with the results of the X-ray diffraction measurements described in the preceding section.

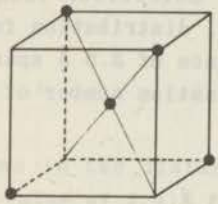

a) tetrahedral coordination

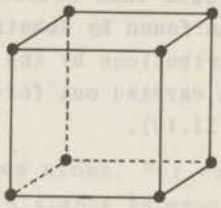

b) octahedral coordination

Figure II.9.

Bernal and Fowler [1] suggested that there are three chief forms of arrangement of the molecules in water:

1) ice-like structure (tridymite structure), present to a certain degree at temperatures below 4°C only,
2) quartz-like structure, predominating at ordinary temperatures,
3) close-packed structure, predominating at high temperatures.

In ice each water molecule is tetrahedrally surrounded by four others at a distance of 2.76 Å. On passing from ice to water there is a diminution of the molar volume from 19.7 to 18.0 ml. This phenomenon is, according to Bernal and Fowler due to a change of the structure from the tridymite to the quartz pattern. With a fixed distance between nearest neighbours this change in structure corresponds to a decrease of 15 % in the molar volume. However, this decrease cannot account for the observed diminution of the molar volume of water if we take into account the increase in the nearest neighbour distance from 2.76 Å to 3.0 Å. The fact that the melting of ice results in a decrease of the molar volume and at the same time is accompanied by an increase of the average distance between neighbouring water molecules indicates that the coordination number in water is higher than that in ice and therefore higher than four. The upper limit of the coordination number calculated from the X-ray diffraction measurements was found to be 7. The coordination number of 6 for the octahedral arrangement is within the limits >4 and <7.

The distance between next-nearest neighbours in the octahedral arrangement is calculated to be 4.25 Å. The X-ray diffraction measurements give indications for a next-nearest neighbour distance of 4.3 Å which is in agreement with the calculated distance.

Although no definite value for the coordination number could be calculated directly from the X-ray diffraction measurements, a further

interpretation of the distribution curves can be attempted. The fact that the O-H distance within the water molecules was detected, suggests that it should also be possible to find the O...H distance in the hydrogen bond between neighbouring water molecules. This distance was found by substracting from the total distribution functions the contributions by the oxygen atoms a distance of 3.0 Å apart; this has been carried out for values of the coordination number of 5 and 7 (figure II.10).

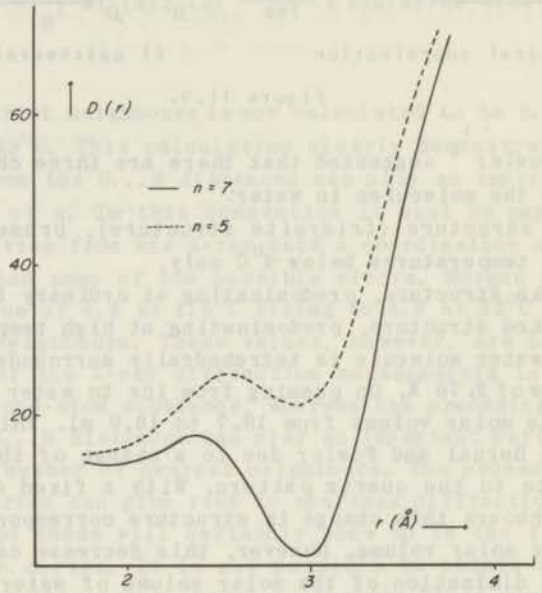

Figure II.10. H_2O, 0°C: total distribution function from which have been substracted the contributions by oxygen atoms 3.0 Å apart.

In the difference curves thus obtained a maximum occurs at about 2.5 Å; the same holds for the distribution curves of water at 25° and 45°C. The position of this maximum somewhat depends on the value of n adopted but it is always in the range 2.45-2.55 Å. This maximum is ascribed to the O...H distance in the hydrogen bond between neighbouring water molecules. As the O-H distance within the water molecules is in the range 0.9-1.0 Å, this O...H distance provides evidence of non-linear hydrogen bonding in liquid water (figure II.11).
With an O...O distance of 3.0 Å, the angle α is in the range 45°-54°. The position of the maximum in the difference curves corresponding to the O...H distance, and hence the angle α, is very sensitive to small

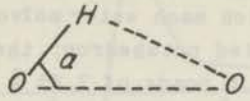

Figure II.11.

variations in the distance between the oxygen atoms. For example, taking a value of 2.9 Å for the average O...O distance between neighbouring water molecules, instead of 3.0 Å, results in an angle α of about 30^{o}. The position of the hydrogen atoms in the hydrogen bond between neighbouring water molecules has been evaluated here in a rather indirect and not very accurate way. Therefore, not too much weight must be attached to the values of α given here.

It is not easy to find the positions of the hydrogen atoms with accuracy by means of X-ray diffraction techniques. This is mainly due to the fact that the scattering power of the hydrogen atom is small compared with that of the oxygen atom. The ratio f_O/f_H equals 8 at zero scattering angle and is still higher at higher scattering angles. A more suitable tool for finding the positions of the hydrogen atoms would have been the application of neutron diffraction techniques (Bacon [26]). As the scattering of neutrons by hydrogen atoms causes a strong diffuse scattering better results are obtainable by replacing the hydrogen atoms by deuterium atoms. The ratio of the scattering power of oxygen and deuterium atoms is about 0.8 which compares favourably with the ratio 8 for the scattering of X-rays.

The non-linear hydrogen bonding can be seen as further evidence in favour of the octahedral arrangement. If we adopt this model for the arrangement of the oxygen atoms, we are left with the problem of fitting the hydrogen atoms into this model. In doing this, the first condition that has to be fulfilled (Orgel [27]) is that the $O\overset{H}{-}H$ angle within the water molecules must equal 104^{o}. The octahedral model was originally proposed with linear hydrogen bonding, involving $O\overset{H}{-}H$ angles of 90^{o}. However, in using the concept of non-linear hydrogen bonding it is possible to place the hydrogen atoms in an octahedral arrangement in such a way that the $O\overset{H}{-}H$ angle equals 104^{o} (for this a minimum value of 7^{o} is required for the angle α).

The arguments put forward in this section then are in favour of an octahedral arrangement of the oxygen atoms with a non-linear hydrogen bonding. It must be realized that the molecular arrangement of liquid water has been discussed here on basis of a crystalline lattice. The proposed model is an idealized one since in a liquid the structure

will be much less rigid. It can only serve as a description of the average arrangement in the immediate neighbourhood of a water molecule.

By taking into account the results of infrared studies on H_2O and $H_2O + D_2O$ mixtures, van Panthaleon van Eck, Mendel and Fahrenfort [3] suggested a model in which each water molecules is surrounded by six others forming a distorted octahedron; the six water molecule form four almost linear O-H...O bonds of 2.85 Å length and two O...O contacts of about 3.6 Å length with the central molecule. The distance of 2.85 Å was obtained from the position of the O-H stretching frequency absorption band by applying a relation between the frequency of maximum absorption and the O-H...O interatomic distance. However, this relation is based upon a model which is incapable of handling bent hydrogen bonds in liquid systems (Lippincott and Schroeder [28]) and in this thesis, therefore, the "structure" of water has been discussed only in terms of the results obtained from the X-ray diffraction measurements.

In the last few years two other models have been proposed for the structure of water. Pople [29] discussed the structure of water in terms of bending of hydrogen bonds only. He restricts his discussion to a model in which n = 4 and takes the required parameters from the distribution curves of water as obtained by Morgan and Warren [4]. The discussion of these distribution curves in section II.2 has revealed that they have to be considered with due reserve and hence the same applies to the parameters used by Pople. Recently Pauling [30] has proposed a model for the structure of water which is analogous to the structure of crystalline gas hydrates. It may be described as involving complexes of 21 water molecules, 20 of which lie at the corners of a pentagonal dodecahedron, each forming three hydrogen bonds with the adjacent neighbours in the dodecahedron and the 21st forming no hydrogen bonds at all and occupying the central position in the dodecahedron. No full details have been published yet, but this structure would seem to contain too high a degree of order to describe the actual arrangement in liquid water.

II.4. X-ray diffraction of KOH solutions

The main purpose of this investigation was to examine whether from the distribution curves of KOH solutions information could be obtained about the hydration number of the potassium ion. KOH was chosen because the OH^--ion is comparable in size and scattering power to the water molecule.

The measurements were carried out at three KOH concentrations, 1.5, 5.0 and 7.5 mole/litre solution. The scattering curves were corrected for absorption and polarization. The final calculated distribution

functions are shown in figure II.12.

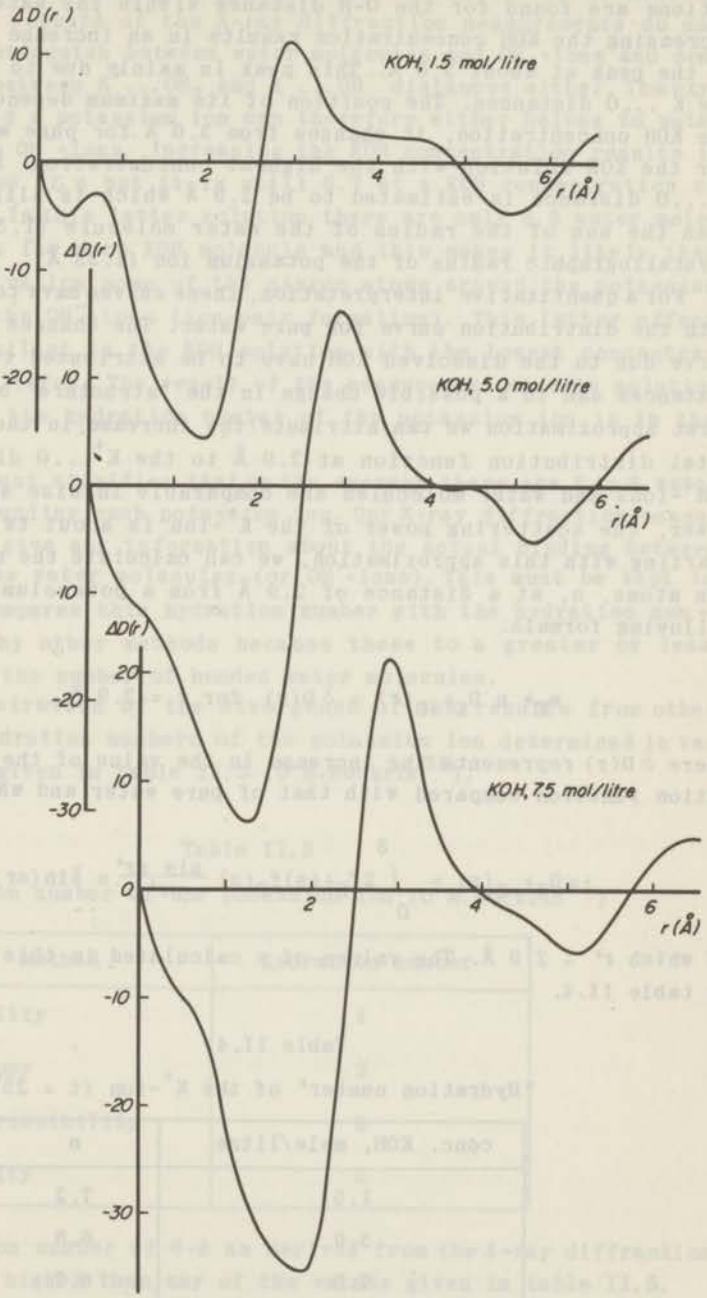

Figure II.12. Distribution curves for KOH solutions at various concentrations.

In these distribution curves, as in the curves for pure water, indications are found for the O-H distance within the water molecules. Increasing the KOH concentration results in an increase in the height of the peak at about 3.0 Å. This peak is mainly due to the O...O and the K^+...O distances. The position of its maximum depends somewhat on the KOH concentration, it changes from 3.0 Å for pure water to 2.9 Å for the KOH solution with the highest concentration. From this the K^+...O distance is estimated to be 2.9 Å which is slightly greater than the sum of the radius of the water molecule (1.50 Å) and the crystallographic radius of the potassium ion (1.33 Å).

For a quantitative interpretation, these curves have to be compared with the distribution curve for pure water. The changes in the latter curve due to the dissolved KOH have to be attributed to the ion-H_2O distances and to a possible change in the "structure" of water. As a first approximation we can attribute the increase in the value of the total distribution function at 2.9 Å to the K^+...O distances only (OH^--ions and water molecules are comparable in size and scattering power, the scattering power of the K^+-ion is about twice as high). Starting with this approximation, we can calculate the number of oxygen atoms, n, at a distance of 2.9 Å from a potassium ion from the following formula:

$$m_{K^+}\, n\, D_{K^+-O}(r) = \delta D(r) \quad \text{for } r = 2.9 \text{ Å}, \qquad (II.9)$$

where $\delta D(r)$ represents the increase in the value of the total distribution function compared with that of pure water and where

$$D_{K^+-O}(r) = \int_0^8 2 f_{K^+}(s) f_O(s) \frac{\sin sr'}{sr'} s \sin(sr) ds \qquad (II.10)$$

in which r' = 2.9 Å. The values of n calculated in this way are given in table II.4.

Table II.4

"Hydration number" of the K^+-ion (t = 25°C)

conc. KOH, mole/litre	n
1.5	7.2
5.0	6.8
7.5	6.7

The figures in table II.4 give us, in first approximation, the number of oxygen atoms around each potassium ion. First of all it must be noted that the results of the X-ray diffraction measurements do not enable us to distinguish between water molecules and OH^--ions and consequently not between $K^+ \ldots OH_2$ and $K^+ \ldots OH^-$ distances either. The oxygen atoms around a potassium ion can therefore either belong to water molecules or to OH^--ions. Increasing the KOH concentration results in a small decrease of n but it is still 6.7 at a KOH concentration of 7.5 mole/litre. In this latter solution there are only 6.5 water molecules available for each KOH molecule and this makes it likely that at this concentration some of the oxygen atoms around the potassium ion belong to the OH^--ions (ion-pair formation). This latter effect will be the smallest in the KOH solution with the lowest concentration (1.5 mole/litre). The result of the measurement on this solution indicates that the hydration number of the potassium ion is in the range 6-8.

This statement signifies that on the average there are 6 to 8 water molecules surrounding each potassium ion. Our X-ray diffraction measurements cannot give any information about the actual binding between the ions and the water molecules (or OH^--ions). This must be kept in mind when one compares this hydration number with the hydration numbers obtained by other methods because these to a greater or less extent measure the number of bonded water molecules.

As an illustration of the divergence of the results from other methods, the hydration numbers of the potassium ion determined in various ways are given in table II.5 (O'M.Bockris[31]).

Table II.5

Hydration number of the potassium ion (O'M.Bockris[31])

method	hydration number
mobility	4
entropy	2
compressibility	3
density	0

The hydration number of 6-8 as derived from the X-ray diffraction measurements is higher than any of the values given in table II.5. However, it is in agreement with the hydration number theoretically calculated by Verwey[32]. According to Verwey the hydration number will

not have a definite value; its average value will generally differ from an integer and will probably lie between 6 and 8 depending upon the size of the ion.

CHAPTER III

OPTICAL REFRACTION OF ELECTROLYTE SOLUTIONS

III.1. Introduction

One of the main problems in the theory of electric polarization is the calculation of the internal field [5], i.e. the electric field acting on a particle (molecule, ion). As this thesis deals with electric polarization at optical frequencies, we shall only consider the case of non-polar, polarizable particles. In the following we shall briefly review some aspects of the Lorentz theory and of the Onsager-Böttcher theory on the internal field.

The older theories on the optical refraction of electrolyte solutions are all based on the Lorentz equation for the internal field [33]. This equation leads to the Lorenz-Lorentz relation:

$$\frac{n^2 - 1}{n^2 + 2} = \frac{4}{3}\pi \sum_i N_i \alpha_i \quad , \qquad \text{(III.1)}$$

n = refractive index,

N_i = number of particles of kind i per unit volume,

α_i = polarizability of particles of kind i.

The Lorenz-Lorentz relation can be written in terms of the molar refraction $[R]$:

$$[R] = \frac{n^2 - 1}{n^2 + 2}\frac{\bar{M}}{d} = \frac{4}{3}\pi N_A \sum_i x_i \alpha_i \quad , \qquad \text{(III.2)}$$

x_i = mole fraction of component i,

$\bar{M} = \sum_i x_i M_i$ with M_i = molecular weight of component i,

N_A = Avogadro's number.

Equation (III.2) predicts that the molar refraction is an additive quantity if the polarizability of the particles is not influenced by the mixing process. The molar refraction of electrolyte solutions turned out to be a non-additive quantity and in addition it was found that the molar refraction of the solute depends upon the concentration. Fajans [34] tried to explain these phenomena by assuming that the pola-

rizability of the particles depends upon the properties of the surrounding medium. However, his theory was incapable of giving a quantitative explanation of the concentration dependence of the molar refraction of dissolved salts.

Onsager's theory [35] on the internal field has been extended and refined by Böttcher [36]. In this theory it is shown that the internal field has different values at the positions of different kinds of particles whereas in using the Lorentz equation for the internal field the assumption is made that this field has the same value at the positions of different kinds of particles. The Onsager-Böttcher theory is based upon a model in which the surroundings of a particle are treated as a continuous, homogeneous medium. This theory leads, for spherical particles, to the following formula:

$$\frac{(n^2 - 1)(2n^2 + 1)}{12\pi n^2} = \sum_i N_i \alpha_i^* , \qquad \text{(III.3)}$$

where

$$\frac{1}{\alpha_i^*} = \frac{1}{\alpha_i} - \frac{1}{r_i^3} \frac{2n^2 - 2}{2n^2 + 1} \qquad \text{(III.4)}$$

and where r_i represents the distance from the centre of the particle to where the surrounding liquid begins; in the following this distance will be called the radius of the particle. If the polarizability and the radius of the particle are molecular constants, a plot of $1/\alpha_i^*$ as a function of $(2n^2 - 2)/(2n^2 + 1)$ will result in a straight line from which it is possible to calculate α_i and r_i. Böttcher [37,38,39], Scholte [40] and Joustra [41] have shown that for a great number of ions such a linear relation between $1/\alpha_i^*$ and $(2n^2 - 2)/(2n^2 + 1)$ exists and this makes Fajans's assumption superfluous in these cases.

A solution of a binary electrolyte in water contains at least three types of particles, i.e. water molecules, cations and anions. In order to calculate the polarizabilities and the radii of ions with the aid of formulae (III.3) and (III.4), it is necessary to know the polarizability and the radius of the water molecules and of one type of ions. The following section deals with the calculation of α_{H_2O} and r_{H_2O}. Assuming these two quantities to be known, we are left with the problem of finding the polarizability and the radius of one type of ions. As the polarizability of the Li^+-ion is extremely small compared with that of most other ions, the method commonly adopted is to take the polarizability of the Li^+-ion equal to zero.

From the polarizability at different wave-lengths it is possible to calculate the pure electronic contribution to the polarizability at infinite wave-length. The values of α_∞ are calculated in this thesis with the extrapolation formula

$$\frac{1}{\alpha_\lambda} = \frac{1}{\alpha_\infty} - \frac{A}{\lambda^2} \qquad \text{(III.5)}$$

which is based on the simple model of a harmonic oscillator [5]. By plotting $1/\alpha_\lambda$ as a function of $1/\lambda^2$ a straight line is obtained which cuts the axis $1/\lambda^2 = 0$ at $1/\alpha_\infty$.

III.2. The radius of the water molecule

Böttcher [37,38,39], Scholte [40] and Joustra [41] have used for the calculation of the polarizabilities and the radii of ions in solution a value of 1.36 Å for the radius of the water molecule. This value was mainly based upon the radius of the water molecule in ice [42]. The most logical way to determine the value to be used in the calculations would be, as indicated by Böttcher [43], to apply formulae (III.3) and (III.4) to pure water. To this end, we can either use the values of the refractive index and density of water at different pressures or at different temperatures. In the following part of this thesis we will examine these two cases.

a) The variation of the refractive index and the density of water with pressure

Rosen [44] gives the values of the refractive index and the density of water at four different pressures and at a number of wave-lengths. His results for λ = 5798 Å are collected in table III.1.

Table III.1

Refractive index and density of water at different pressures (Rosen [44])

$t = 25^oC$ λ = 5798 Å

p (atm)	d	n
1	0.9971	1.3330
500	1.0185	1.3401
1000	1.0381	1.3462
1500	1.0559	1.3516

The values of $1/\alpha^*$ and $(2n^2 - 2)/(2n^2 + 1)$ as calculated from these data are plotted in figure III.1; for other wave-lengths a similar result is obtained.

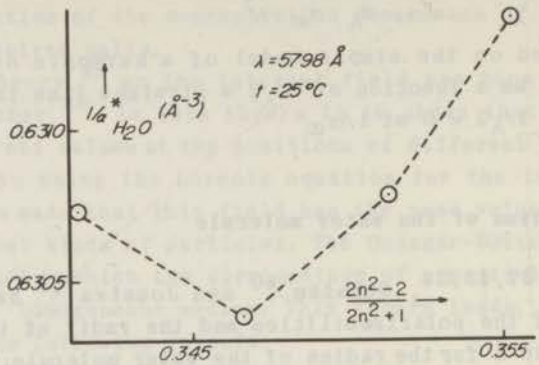

Figure III.1. $1/\alpha^*$ as a function of $(2n^2 - 2)/(2n^2 + 1)$ for water at different pressures.

Obviously it is impossible to calculate from these data a radius for the water molecule. No definite conclusions can be drawn from these results as the number of experimental points is small and as it is difficult to get an impression of the accuracy of the measurements.

b) *The variation of the refractive index and the density of water with temperature*

The refractive index of water in the temperature range 0^o - 60^oC at various wave-lengths has been measured with great accuracy by Tilton and Taylor[6]. The values of $1/\alpha^*$ and $(2n^2 - 2)/(2n^2 + 1)$ for λ = 5893 Å as calculated * from their data are plotted in figure III.2.
It can be seen from this graph that there exists no linear relation between these two quantities; the deviations from linearity are most pronounced in the temperature range 0^o - 30^oC. For other wave-lengths a similar result is obtained. An "apparent radius" of the water molecule has been calculated from the slope of the curve; this radius is of course a function of the temperature (table III.2).

The Onsager-Böttcher theory is based upon a model in which the surroundings of a particle are treated as a continuous, homogeneous medium. From our X-ray diffraction measurements on water it could be concluded that a certain structure exists in liquid water. It could also be concluded that an increase in temperature corresponds to a

* The density of water was taken from tables given by Dorsey [45].

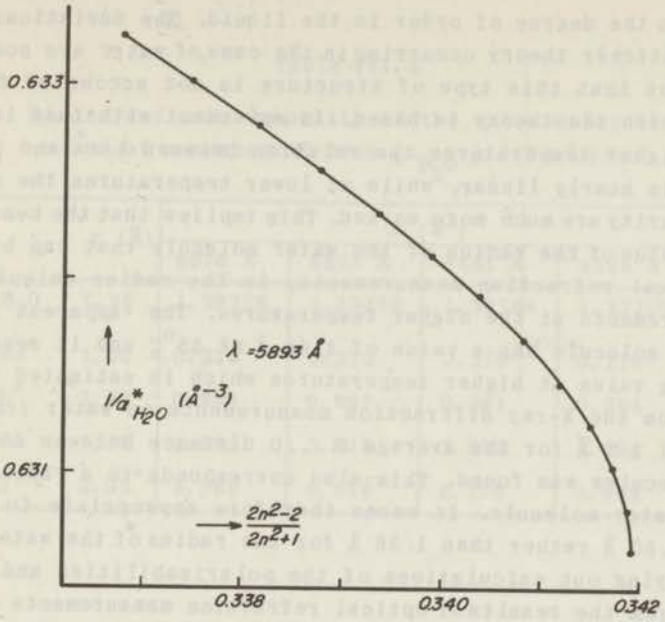

Figure III.2. $1/\alpha$ as a function of $(2n^2 - 2)/(2n^2 + 1)$ for water at different temperatures.

Table III.2

"Apparent radius" of the water molecule

t °C	r (Å)
5	0.78
10	0.96
15	1.09
20	1.16
25	1.23
30	1.28
35	1.33
40	1.36
45	1.39
50	1.43
55	1.45

decrease in the degree of order in the liquid. The deviations from the Onsager-Böttcher theory occurring in the case of water are possibly due to the fact that this type of structure is not accounted for in the model on which the theory is based. In agreement with this is the fact that at higher temperatures the relation between $1/\alpha^*$ and $(2n^2 - 2)/(2n^2 + 1)$ is nearly linear, while at lower temperatures the deviations from linearity are much more marked. This implies that the best estimate for the value of the radius of the water molecule that can be obtained from optical refraction measurements, is the radius calculated from the measurements at the higher temperatures. The "apparent radius" of the water molecule has a value of 1.45 Å at 55°C and it seems to have a limiting value at higher temperatures which is estimated to be about 1.5 Å. From the X-ray diffraction measurements on water (chapter II) a value of 3.0 Å for the average O....O distance between neighbouring water molecules was found. This also corresponds to a radius of 1.5 Å for the water molecule. It seems therefore appropriate to adopt the value of 1.50 Å rather than 1.36 Å for the radius of the water molecule when carrying out calculations of the polarizabilities and the radii of ions from the results of optical refraction measurements on aqueous electrolyte solutions.

The results of our measurements of the refractive indices and the densities of a number of aqueous electrolyte solutions are given in chapter IV. From these are calculated the polarizabilities and the radii of a number of ions, using the value of 1.50 Å for the radius of the water molecule. The results of the measurements of Joustra [41] have been used to calculate the polarizabilities and the radii of those ions for which these values were needed in the calculations just mentioned. Joustra's original results, based upon the value of 1.36 Å for the radius of the water molecule, are collected in table III.3 whereas the results based upon the value of 1.50 Å for the radius of the water molecule are collected in table III.4. It must be emphasized that if the value of 1.50 Å is used the relation between $1/\alpha^*$ of these ions and $(2n^2 - 2)/(2n^2 + 1)$ is again linear.

Table III.3

Radius and polarizability of the water molecule and of a number of ions (r_{H_2O} = 1.36 Å)

	r (Å)	α (Å^3)			
		6678 Å	5893 Å	5461 Å	4358 Å
H_2O	1.36	1.29756	1.30349	1.30764	1.32359
Na^+	1.00	0.210	0.210	0.210	0.210
K^+	1.17	0.889	0.891	0.891	0.894
Cl^-	1.82	2.993	3.013	3.029	3.094
I^-	2.52*	6.566	6.646	6.708	6.984

Table III.4

Radius and polarizability of the water molecule and of a number of ions (r_{H_2O} = 1.50 Å)

	r (Å)	α (Å^3)			
		6678 Å	5893 Å	5461 Å	4358 Å
H_2O	1.50	1.35807	1.36488	1.36963	1.38801
Na^+	1.00	0.215	0.215	0.215	0.215
K^+	1.32	0.948	0.949	0.950	0.953
Cl^-	2.10	3.258	3.283	3.303	3.385
I^-	2.70*	6.992	7.085	7.161	7.477

* As calculated from potassium iodide solutions.

CHAPTER IV

RESULTS AND DISCUSSION OF OPTICAL REFRACTION MEASUREMENTS

IV.1. Experimental

The experimental technique has recently been described in great detail by Joustra [41] and therefore only a short description will be given here.

a) Chemicals

In the present investigations use was made of the following chemicals:

Sodium nitrate, potassium nitrate, silver nitrate and potassium iodide, p.a. grade (Merck-Darmstadt).

Mercuric iodide (Merck-Darmstadt), twice recrystallized from n-amyl alcohol.

The salts were dried for about six hours in a "drying pistol" (pressure 10 mm Hg, temperature 200°C), using phosphorous pentoxide as a drying agent. The solutions were made up by dissolving exactly known quantities of the dried salts in water and determining the weight of the solutions. The water was twice distilled from an all-quartz apparatus and boiled out before making up the solutions in order to remove the dissolved gases.

b) Measurement of the density

The densities of the solutions were determined with the aid of Aubry pycnometers (volume about 10 ml), which were calibrated with water. All measurements were made at a temperature of $25^{\circ}.00 \pm 0^{\circ}.02$ C. The density of each solution was determined in duplicate. The reproducibility was two units in the fifth decimal place, except for the concentrated silver nitrate solutions and for the concentrated solutions of potassium iodide + mercuric iodide where it was about five units in the fifth decimal place.

c) Measurement of the refractive index

The refractive indices were determined with the aid of an Abbe refractometer (precision refractometer manufactured by the Bausch and Lomb Comp., type 33.45.03). Measurements were made at four different wave-lengths, viz. 6678 Å (He c), 5893 Å (Na D), 5461 Å (Hg e) and

4358 Å (Hg g). The temperature was maintained at $25^{\circ}.00 \pm 0^{\circ}.02$ C. The reproducibility of the refractive index measurements depended somewhat on the wave-length due to the unequal sensitivity of the eye to light of different wave-lengths. It was about three units in the fifth decimal place for the wave-lengths 5893 Å and 5461 Å and about six units in the fifth decimal place for the wave-lengths 6678 Å and 4358 Å.

IV.2. Optical refraction of sodium nitrate and potassium nitrate solutions *

Optical refraction measurements on aqueous sodium nitrate solutions were made in order to calculate the radius and the polarizability of the nitrate ion. The nitrate ion, having a planar structure in the form of a centred equilateral triangle [46], was chosen as an example of a non-spherical ion. The derivation of formulae (III.3) and (III.4) is based upon a model in which the particles are supposed to have spherical symmetry. However, Scholte [40] has shown that in the case of ellipsoidal particles, which is a fair enough approximation for the nitrate ion, formulae (III.3) and (III.4) still hold. The polarizability calculated with the aid of these formulae equals, for ellipsoidal particles, the mean value of the polarizabilities in the direction of the three axes of the particle.

In order to examine whether the polarizability of the nitrate ion is influenced by the cation, it has been calculated from measurements of the optical refraction of aqueous potassium nitrate solutions as well.

The experimental results for the sodium nitrate solutions are given in table IV.1. In this and the following tables d denotes the density of the solutions and m the concentration in mol/1000 g water.

In figure IV.1, $1/\alpha^{*}_{NO_3^-}$ is plotted as a function of $(2n^2 - 2)/(2n^2 + 1)$. The radius of the nitrate ion has been calculated from the slopes of the resulting straight lines (table IV.2). The values of $\alpha_{NO_3^-}$ given in table IV.1 have been calculated with the average value of 2.20 Å for the radius of the nitrate ion. The average value of $\alpha_{NO_3^-}$ for each wave-length together with the extrapolated value for infinite wave-length is given in table IV.2.

---

* The author's thanks are due to Mr. J.A.C.M. van der Beek for his assistance in carrying out the measurements.

Table IV.1

Polarizability of the NO_3^--ion from $NaNO_3$ solutions (t = 25°C)

m	d	6678 Å		5893 Å		5461 Å		4358 Å	
		n	α (Å^3)	n	α (Å^3)	n	α (Å^3)	n	α (Å^3)
1.6233	1.08080	1.34372	3.954	1.34595	3.979	1.34760	4.007	1.35397	4.109
2.0895	1.10260	1.34700	3.950	1.34930	3.979	1.35098	4.006	1.35754	4.110
2.4294	1.11785	1.34927	3.951	1.35161	3.980	1.35335	4.009	1.36002	4.112
2.9635	1.14116	1.35273	3.950	1.35515	3.982	1.35690	4.008	1.36374	4.111
3.9634	1.18190	1.35858	3.949	1.36112	3.982	1.36298	4.010	1.37008	4.109
4.3893	1.19807	1.36084	3.949	1.36338	3.981	1.36525	4.007	1.37252	4.109
5.0759	1.22339	1.36436	3.948	1.36696	3.980	1.36887	4.006	1.37635	4.108
5.6096	1.24210	1.36696	3.949	1.36954	3.979	1.37149	4.005	1.37914	4.108
6.4391	1.26984	1.37073	3.949	1.37346	3.980	1.37543	4.007	1.38331	4.111
6.9756	1.28664	1.37296	3.950	1.37566	3.980	1.37770	4.007	1.38567	4.109
7.9042	1.31465	1.37670	3.951	1.37948	3.982	1.38153	4.007	1.38971	4.109
8.9842	1.34478	1.38064	3.952	1.38347	3.983	1.38566	4.008	1.39401	4.111
9.6632	1.36273	1.38288	3.950	1.38577	3.982	1.38789	4.007	1.39654	4.111

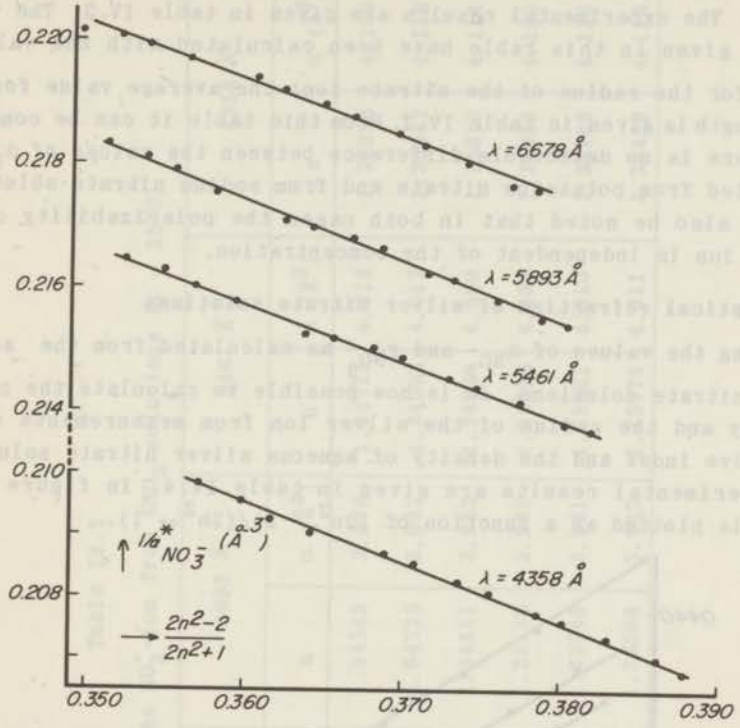

Figure IV.1. Radius of the nitrate ion from sodium nitrate solutions.

Table IV.2

Radius and polarizability of the NO_3^--ion

λ (Å)	$NaNO_3$ solutions		KNO_3 solutions
	r (Å)	α (Å^3)	α (Å^3)
6678	2.22	3.950	3.951
5893	2.16	3.981	3.981
5461	2.22	4.007	4.010
4358	2.20	4.110	4.112
∞		3.838	

The polarizability of the nitrate ion has been calculated from measurements of the optical refraction of potassium nitrate solutions as well. The experimental results are given in table IV.3. The values of $\alpha_{NO_3^-}$ given in this table have been calculated with the value of 2.20 Å for the radius of the nitrate ion; the average value for each wave-length is given in table IV.2. From this table it can be concluded that there is no detectable difference between the values of $\alpha_{NO_3^-}$ as calculated from potassium nitrate and from sodium nitrate solutions. It must also be noted that in both cases the polarizability of the nitrate ion is independent of the concentration.

IV.3. Optical refraction of silver nitrate solutions

Using the values of $\alpha_{NO_3^-}$ and $r_{NO_3^-}$ as calculated from the aqueous sodium nitrate solutions, it is now possible to calculate the polarizability and the radius of the silver ion from measurements of the refractive index and the density of aqueous silver nitrate solutions. The experimental results are given in table IV.4. In figure IV.2, $1/\alpha^*_{Ag^+}$ is plotted as a function of $(2n^2 - 2)/(2n^2 + 1)$.

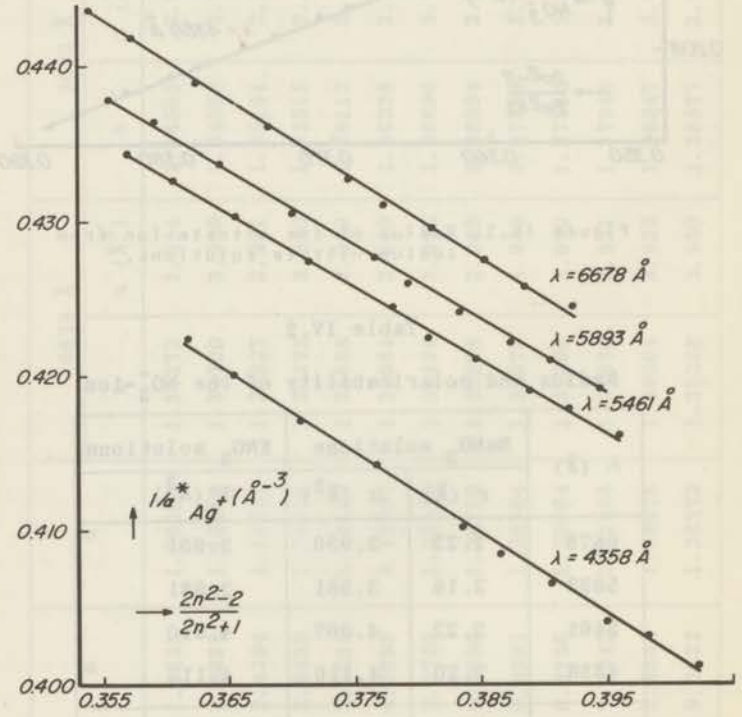

Figure IV.2. Radius of the silver ion from $AgNO_3$ solutions.

Table IV.3

Polarizability of the NO_3^--ion from KNO_3 solutions (t = 25°C)

m	d	6678 Å		5893 Å		5461 Å		4358 Å	
		n	α (Å^3)	n	α (Å^3)	n	α (Å^3)	n	α (Å^3)
1.5983	1.08724	1.34321	3.951	1.34543	3.979	1.34711	4.013	1.35336	4.109
1.8668	1.10092	1.34508	3.952	1.84735	3.982	1.34902	4.012	1.35542	4.116
1.9789	1.10652	1.34585	3.953	1.34811	3.982	1.34977	4.009	1.35618	4.111
2.4625	1.12999	1.34895	3.948	1.35130	3.982	1.35296	4.006	1.35953	4.109
2.8152	1.14632	1.35109	3.948	1.35346	3.981	1.35521	4.010	1.36188	4.113
3.2290	1.16503	1.35362	3.952	1.35598	3.982	1.35776	4.011	1.36459	4.116

Table IV.4

Polarizability of the Ag^+-ion from $AgNO_3$ solutions (t = 25°C)

m	d	6678 Å		5893 Å		5461 Å		4358 Å	
		n	α (Å^3)	n	α (Å^3)	n	α (Å^3)	n	α (Å^3)
1.1819	1.15531	1.34969	1.611	1.35207	1.624	1.35375	1.632	1.36027	1.658
1.4809	1.19321	1.35427	1.611	1.35670	1.623	1.35844	1.632	1.36518	1.659
1.9424	1.24979	1.36104	1.613	1.36356	1.624	1.36536	1.631	1.37242	1.660
2.5049	1.31622	1.36893	1.613	1.37159	1.625	1.37345	1.631	1.38086	1.659
3.1630	1.39068	1.37777	1.613	1.38052	1.624	1.38249	1.630	1.39038	1.662
3.4621	1.42322	1.38162	1.614	1.38141	1.625	1.38647	1.633	1.39452	1.663
3.8994	1.46973	1.38706	1.613	1.38996	1.624	1.39203	1.630	1.40039	1.662
4.3809	1.51925	1.39280	1.613	1.39586	1.624	1.39800	1.630	1.40667	1.663
4.7629	1.55751	1.39739	1.613	1.40038	1.623	1.40257	1.629	1.41143	1.661
5.2616	1.60582	1.40297	1.611	1.40611	1.622	1.40835	1.629	1.41751	1.660

The radius of the silver ion has been calculated from the slopes of the resulting straight lines (table IV.5). The average value of the radius, 1.26 Å, is exactly the same as the crystallographic radius given by Pauling [47]. The values of α_{Ag^+} given in table IV.4, calculated with the average value of 1.26 Å for the radius of the silver ion, clearly show that the polarizability of the silver ion is independent of the concentration of the silver nitrate solutions. The average value of α_{Ag^+} for each wave-length together with the extrapolated value for infinite wave-length is given in table IV.5.

Table IV. 5

Radius and polarizability of the Ag^+-ion

λ(Å)	r (Å)	α(Å^3)
6678	1.25	1.613
5893	1.27	1.624
5461	1.28	1.631
4358	1.23	1.661
∞		1.580

In applying the Onsager-Böttcher theory to the optical refraction of aqueous silver nitrate solutions, it has been assumed that this electrolyte is completely dissociated. However, it is known from conductivity measurements (Campbell and Kartzmark [48]) that the dissociation is incomplete; at m = 3.4, for example, the degree of dissociation is only 0.84. This incomplete dissociation does not show up in the relation between $1/\alpha^*_{Ag^+}$ and $(2n^2 - 2)/(2n^2 + 1)$. The question as to how far the Onsager-Böttcher theory can give information about the association of ions in solution will be further examined in the following section.

IV.4. Optical refraction of solutions of potassium iodide + mercuric iodide

In solutions containing Hg^{2+}-ions and halide ions a number of mercuric-halide complexes can be formed. The distribution of the mercuric ions over the various complexes depends strongly on the concentration of the halide ions. The equilibria existing between these complexes have been investigated by Sillén [49]. From his electrometric

Table IV.6

Polarizability of the HgI_4^{2-}-ion from aqueous solutions of HgI_2 + KI (t = 25°)

m_{KI}	m_{HgI_2}	d	6678 Å		5893 Å		5461 Å		4358 Å	
			n	α (Å^3)	n	α (Å^3)	n	α (Å^3)	n	α (Å^3)
0.7847	0.2845	1.18618	1.36170	29.93	1.36487	30.51	1.36725	31.00	1.37747	33.33
0.7955	0.2877	1.18836	1.36214	29.97	1.36529	30.54	1.36766	31.01	1.37793	33.34
1.3243	0.2700	1.23569	1.37048	29.98	1.37378	30.54	1.37630	31.03	1.38709	33.38
1.3310	0.4881	1.30686	1.38200	29.98	1.38580	30.54	1.38874	31.00	1.40211	33.36
2.3800	0.3425	1.35619	1.39106	29.99	1.39491	30.57	1.39781	31.02	1.41073	33.37
1.8887	0.5326	1.37102	1.39301	29.98	1.39711	30.54	1.40029	31.01	1.41484	33.37
2.0088	0.6473	1.41591	1.40042	29.97	1.40483	30.53	1.40825	30.99	1.42426	33.35
2.3164	0.5606	1.41601	1.40061	29.94	1.40494	30.51	1.40828	30.98	1.42363	33.34
2.6048	0.7331	1.48930	1.41302	29.98	1.41777	30.54	1.42150	31.00	1.43914	33.37
2.7455	0.7138	1.49458	1.41392	29.98	1.41868	30.53	1.42241	30.99	1.43993	33.36
2.2451	0.9354	1.51830	1.41748	29.96	1.42258	30.52	1.42665	30.98	1.44623	33.35
2.2761	1.0464	1.55169	1.42289	29.93	1.42832	30.50	1.43257	30.96	1.45344	33.33
3.2473	0.8430	1.56783	1.42635	29.97	1.43153	30.53	1.43563	30.99	1.45507	33.37
3.4134	1.0738	1.63965	1.43846	29.99	1.44423	30.56	1.44876	31.01	1.47090	33.39
3.1135	1.1688	1.64407	1.43891	29.96	1.44479	30.52	1.44944	30.98	1.47237	33.35
3.4159	1.4943	1.74605	1.45623	29.95	1.46289	30.51	1.46819	30.97	1.49486	33.33
4.3852	1.2726	1.75100	1.45751	29.98	1.46391	30.55	1.46898	31.00	1.49406	33.40
4.7665	1.6983	1.87048	1.47791	29.97	1.48526	30.53	1.49119	31.00	1.52096	33.39
5.1759	2.1878	1.99504	1.49938	29.96	1.50782	30.53	1.51458	30.99	1.54956	33.38

investigation it follows that all the HgI_2 is converted into HgI_4^{2-}-ions in solutions of HgI_2 + KI in which $c_{KI} > 2c_{HgI_2}$ (c = concentration in mol/litre solution). The polarizability and the radius of the HgI_4^{2-}-ion have been calculated from measurements of the refractive indices and the densities of aqueous solutions of potassium iodide + mercuric iodide in which $c_{KI} - 2c_{HgI_2} > 0.15$ mol/litre. The experimental results are given in table IV.6.

A plot of $1/\alpha^*_{HgI_4^{2-}}$ as a function of $(2n^2 - 2)/(2n^2 + 1)$ reveals the linear relation existing between these two quantities (figure IV.3). The radius of the HgI_4^{2-}-ion has been calculated from the slopes of the straight lines (table IV.7). The values of the polarizability of the HgI_4^{2-}-ion given in table IV.6 were calculated with the average value of 3.79 Å for $r_{HgI_4^{2-}}$. The average value of the polarizability for each wave-length together with the extrapolated value for infinite wave-length is given in table IV.7.

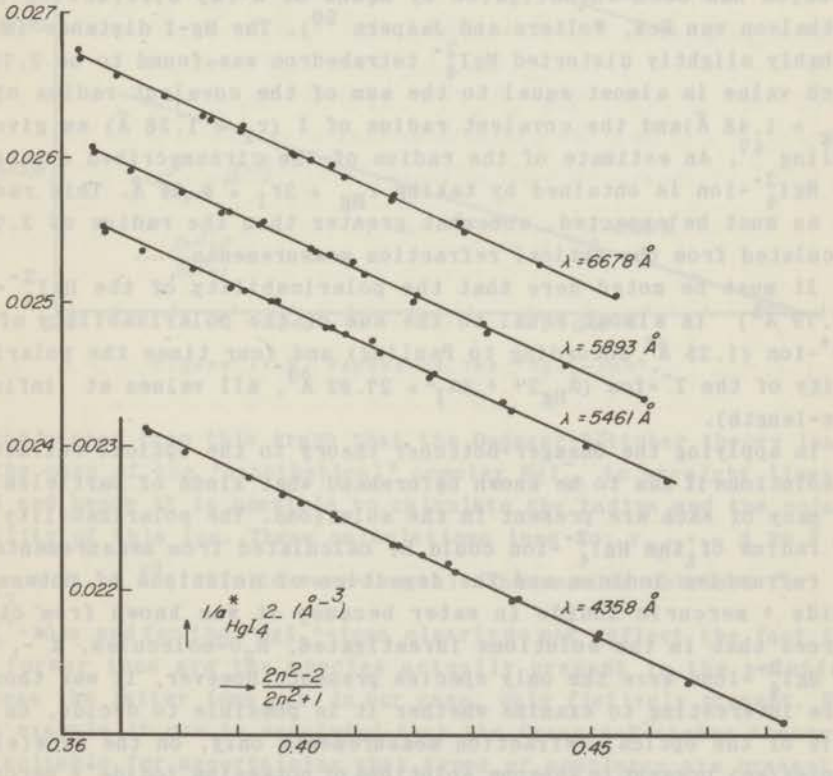

Figure IV.3. Radius of the HgI_4^{2-}-ion from solutions of HgI_2 + KI.

Table IV.7

Radius and polarizability of the HgI_4^{2-}-ion

λ (Å)	r (Å)	α (Å^3)
6678	3.79	29.97
5893	3.80	30.53
5461	3.81	31.00
4358	3.77	33.36
∞		27.79

The structure of a number of mercuric-halide complexes in aqueous solution has been investigated by means of X-ray diffraction (van Panthaleon van Eck, Wolters and Jaspers [50]). The Hg-I distance in the probably slightly distorted HgI_4^{2-} tetrahedron was found to be 2.78 Å, which value is almost equal to the sum of the covalent radius of Hg (r_{Hg} = 1.48 Å)and the covalent radius of I (r_I = 1.28 Å) as given by Pauling [47]. An estimate of the radius of the circumscribed sphere of the HgI_4^{2-}-ion is obtained by taking $r_{Hg} + 2r_I$ = 4.04 Å. This radius is, as must be expected, somewhat greater than the radius of 3.79 Å calculated from the optical refraction measurements.

It must be noted here that the polarizability of the HgI_4^{2-}-ion (27.79 Å^3) is almost equal to the sum of the polarizability of the Hg^{2+}-ion (1.25 Å^3 according to Pauling) and four times the polarizability of the I^--ion ($\alpha_{Hg^{2+}} + 4\alpha_{I^-}$ = 27.92 Å^3, all values at infinite wave-length).

In applying the Onsager-Böttcher theory to the optical refraction of solutions it has to be known beforehand what kinds of particles and how many of each are present in the solutions. The polarizability and the radius of the HgI_4^{2-}-ion could be calculated from measurements of the refractive indices and the densities of solutions of potassium iodide + mercuric iodide in water because it was known from other sources that in the solutions investigated, H_2O-molecules, K^+-, I^-- and HgI_4^{2-}-ions were the only species present. However, it was thought to be interesting to examine whether it is possible to decide, on the basis of the optical refraction measurements only, on the type(s) of complex(es) present in aqueous solutions of potassium iodide + mercuric iodide. In order to do so, the experimental results were interpreted in terms of the complex HgI_3^-. According to the results of Sillén [49]

this complex is present in solutions of KI + HgI_2 at low KI concentrations but not in the solutions investigated here: in these solutions all the Hg^{2+}-ions have formed HgI_4^{2-}-ions.

In figure IV.4, $1/\alpha^*_{HgI_3^-}$ is plotted as a function of $(2n^2 - 2)/(2n^2 + 1)$.

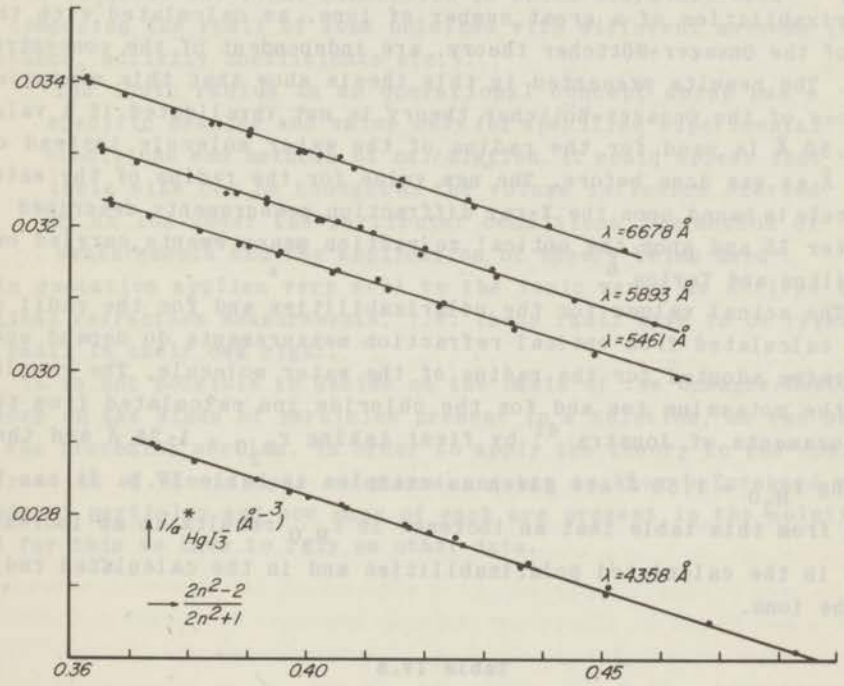

Figure IV.4. Radius of the "HgI_3^--ion".

It can be seen from this graph that the Onsager-Böttcher theory leads, in the case of the "hypothetical" complex HgI_3^-, to straight lines as well and hence it is possible to calculate the radius and the polarizability of this ion. These calculations lead to: $r_{HgI_3^-} = 3.39$ Å and $\alpha_{HgI_3^-} = 21.19$ Å^3 (infinite wave-length). The results obtained for the HgI_4^{2-}-ions and for the "HgI_3^-"-ions clearly do not reflect the fact that the former ions are the species actually present in the solutions whereas the latter ions are, in our case, only fictively present. From this example it can be concluded that the Onsager-Böttcher theory is not suitable for ascertaining what types of complexes are present in solutions.

IV.5. Discussion

The Onsager-Böttcher theory gives a satisfactory explanation of the non-additivity of the molar refraction of electrolyte solutions. The assumption Fajans [34] had to make to explain this non-additivity are therefore superfluous. This has been demonstrated by Böttcher [37,38,39], Scholte [40] and Joustra [41]. These authors showed that the polarizabilities of a great number of ions, as calculated with the aid of the Onsager-Böttcher theory, are independent of the concentration. The results presented in this thesis show that this essential success of the Onsager-Böttcher theory is not invalidated if a value of 1.50 Å is used for the radius of the water molecule instead of 1.36 Å as was done before. The new value for the radius of the water molecule is based upon the X-ray diffraction measurements described in chapter II and upon the optical refraction measurements carried out by Tilton and Taylor [6].

The actual values for the polarizabilities and for the radii of ions calculated from optical refraction measurements do depend upon the value adopted for the radius of the water molecule. The results for the potassium ion and for the chloride ion calculated from the measurements of Joustra [41] by first taking r_{H_2O} = 1.36 Å and then taking r_{H_2O} = 1.50 Å are given as examples in table IV.8. It can be seen from this table that an increase in r_{H_2O} results in an increase both in the calculated polarizabilities and in the calculated radii of the ions.

Table IV.8

Radius and polarizability of the potassium and the chloride ion

r_{H_2O}	K^+		Cl^-	
	r (Å)	α_∞ (Å^3)	r (Å)	α_∞ (Å^3)
1.36	1.17	0.886	1.82	2.922
1.50	1.32	0.944	2.10	3.169
	r_C =1.33		r_C =1.81	

The radii of the potassium ion and of the chloride ion as calculated from the optical refraction measurements are compared in this table with the crystallographic radii, r_C, of these ions. The agreement is

excellent if for the radius of the water molecule we adopt a value of 1.50 Å in the case of the potassium ion and a value of 1.36 Å in the case of the chloride ion. It must be emphasized, however, that in view of the simple model on which the Onsager-Böttcher theory is based one should not expect an exact agreement of the calculated radii with the crystallographic radii of the ions. In connection with this, it is useful to quote the final conclusion to which Stern and Amis [51] come by comparing the radii of ions obtained with different methods (conductance, activity coefficients etc.):

> "The ionic radius is an operational concept which has a specific meaning and value only for specified experimental conditions and methods of calculation. It would appear that ionic size can be thought as the volume influence exerted by an ion under the particular conditions, the method of measurements and the application of theory being used".

This quotation applies very well to the ionic radii as derived from optical refraction measurements, i.e. these radii have to be regarded as radii in their own right.

It is not possible to decide on the basis of the Onsager-Böttcher theory on the kinds of particles present in a solution, as was shown in the preceding section. In order to apply the theory to the optical refraction of electrolyte solutions one has to know beforehand what kinds of particles and how many of each are present in the solutions and for this we have to rely on other data.

SAMENVATTING

In dit proefschrift zijn enige onderzoekingen beschreven die verricht werden aan water en aan oplossingen van elektrolyten in water. Het experimentele werk omvatte metingen van de röntgen-diffractie en van de optische refractie. De röntgen-diffractiemetingen moesten dienen om informatie te verkrijgen omtrent de in vloeistoffen voorkomende structuur. Deze structuur wordt juist buiten beschouwing gelaten in de Onsager-Böttcher theorie, welke in dit proefschrift gebruikt werd voor de interpretatie van de optische refractiemetingen. Uit metingen van brekingsindices en dichtheden van elektrolytoplossingen kunnen met behulp van deze theorie de polariseerbaarheid en de straal van ionen berekend worden.

In hoofdstuk I wordt beschreven hoe uit röntgen-diffractiemetingen aan vloeistoffen de verdelingsfuncties berekend kunnen worden. Speciale aandacht wordt hier ook besteed aan de berekening van de schaalfactor die gebruikt moet worden voor de omrekening van de waargenomen intensiteiten op een absolute schaal.

In het tweede hoofdstuk worden de resultaten van de röntgen-diffractiemetingen besproken. Teneinde de experimentele techniek en de rekenmethodiek te toetsen werden eerst metingen verricht aan amorf SiO_2. De uit deze metingen berekende Si-O afstand blijkt in overeenstemming te zijn met de uit de literatuur bekende waarden. Bovendien kon worden berekend dat in amorf SiO_2 ieder siliciumatoom omgeven is door vier zuurstofatomen.

De röntgen-diffractiemetingen aan water werden verricht bij 0^{o}, 25^{o} en 45^{o}C. Van de in deze vloeistof voorkomende interatomaire afstanden werd o.a. de O-H afstand in de watermoleculen gevonden. Tevens werden aanwijzingen gevonden voor het optreden van niet-lineaire waterstofbruggen in water. Nagegaan werd met welk model voor de "structuur" van water de resultaten het beste in overeenstemming zijn. Dit bleek het model te zijn waarin ieder zuurstofatoom octaëdrisch omringd is door zes zuurstofatomen.

Verder werd nagegaan of het mogelijk is om met behulp van röntgen-diffractiemetingen gegevens te verkrijgen over de hydratatiegetallen van ionen in oplossing. Uit metingen aan KOH-oplossingen van verschillende concentraties werd voor het K^{+}-ion een hydratatiegetal van 6-8 gevonden. Onder hydratiegetal moet hier dan worden verstaan het gemiddelde aantal watermoleculen dat zich om een K^{+}-ion bevindt; de röntgen-diffractiemetingen geven geen informatie omtrent de binding tus-

sen de ionen en de watermoleculen (of OH^--ionen).

Een belangrijke grootheid nodig voor de berekening van de polariseerbaarheid en de straal van ionen uit refractiemetingen aan oplossingen van elektrolyten in water is de straal van het watermolecule. Door andere onderzoekers werd hiervoor steeds een waarde van 1.36 Å gebruikt, welke voornamelijk gebaseerd was op de straal van het watermolecule in ijs. In het derde hoofdstuk van dit proefschrift worden argumenten naar voren gebracht om in plaats van 1.36 Å de waarde 1.50 Å voor de straal van het watermolecule te gebruiken. Deze argumenten zijn gebaseerd op de in het tweede hoofdstuk beschreven röntgen-diffractiemetingen aan water en op de temperatuur-afhankelijkheid van de brekingsindex van water, zoals deze uit de literatuur bekend is. Bij de berekeningen in dit proefschrift werd steeds de waarde 1.50 Å gebruikt.

In het vierde hoofdstuk worden de resultaten vermeld van de verrichte refractiemetingen. De polariseerbaarheid van het NO_3^--ion werd berekend uit metingen aan $NaNO_3$- en KNO_3-oplossingen en bleek onafhankelijk van het kation te zijn. De uit deze metingen bepaalde polariseerbaarheid en straal van het NO_3^--ion werden gebruikt om uit refractiemetingen aan $AgNO_3$-oplossingen de polariseerbaarheid en de straal van het Ag^+-ion te berekenen. Uit de literatuur is bekend dat de dissociatie van $AgNO_3$ in waterige oplossing onvolledig is, hetgeen echter niet tot uiting kwam in de resultaten van de refractiemetingen. Dit probleem van associatie in oplossing werd nader onderzocht aan oplossingen van KJ + HgJ_2 in water. Het is bekend dat in oplossingen waarin de concentratie van het KJ tweemaal zo groot is als die van het HgJ_2, al het HgJ_2 omgezet wordt in het complexe ion HgJ_4^{2-}. De polariseerbaarheid en de straal van dit ion werden berekend uit refractiemetingen aan oplossingen van KJ + HgJ_2 die aan deze voorwaarde voldeden. Daarna werd nagegaan of de refractiemetingen zelf ook aanleiding geven te concluderen tot de aanwezigheid van het HgJ_4^{2-}-ion in de onderzochte oplossingen. Dit bleek niet het geval te zijn; de resultaten van de metingen zouden even goed interpreteerbaar zijn als we zouden aannemen dat in de oplossingen niet het HgJ_4^{2-}-ion doch het "hypothetische" HgJ_3^--ion aanwezig is. Teneinde de Onsager-Böttcher theorie te gebruiken voor de berekening van de polariseerbaarheid en de straal van complexe ionen moet dus langs andere weg eerst vastgesteld worden welke ionen in de oplossingen voorkomen.

REFERENCES

1. J.D. Bernal and R.H. Fowler, J.Chem.Phys. **1**, 515 (1933).
2. C.L. van Panthaleon van Eck, H. Mendel and W. Boog, Discussions Faraday Soc. **24**, 200 (1957).
3. C.L. van Panthaleon van Eck, H. Mendel and J. Fahrenfort, Proc.Roy.Soc. (London) **A 247**, 472 (1958).
4. J. Morgan and B.E. Warren, J.Chem.Phys. **6**, 666 (1938).
5. C.J.F. Böttcher, Theory of Electric Polarisation, Elsevier Publ.Comp., Amsterdam, 1952.
6. L.W. Tilton and J.K. Taylor, J. Research Natl. Bur. Standards **20**, 419 (1938).
7. P. Debye, Ann. Physik **46**, 809 (1915).
8. F. Zernicke and J.A. Prins, Z. Physik **41**, 184 (1927).
9. R.W. James, The Optical Principles of the Diffraction of X-rays, G. Bell and Sons Ltd., London, 1948.
10. B.E. Warren, H. Krutter and O. Morningstar, J.Am. Ceramic Soc. **19**, 202 (1936).
11. G.W. Brady and J.T. Krause, J. Chem. Phys. **27**, 304 (1957).
12. G.W. Brady, J.Chem.Phys. **28**, 464 (1958).
13. J. Krogh-Moe, Acta Cryst. **9**, 951 (1956).
14. N. Norman, Acta Cryst. **10**, 370 (1957).
15. K. Sagel, Tabellen zur Röntgenstrukturanalyse, Springer Verlag, Berlin, 1958.
16. R. McWeeny, Acta Cryst. **4**, 513 (1951).
17. J. Berghuis, Y.M. Haanappel, M. Potters, B.O. Loopstra, C.H. MacGillavry and A.L. Veenendaal, Acta Cryst. **8**, 478 (1955).
18. M.E. Milberg and A.D. Brailsford, Acta Cryst. **11**, 672 (1958).
19. A.H. Compton and S.K. Allison, X-rays in Theory and Experiment, D. van Nostrand Comp., New York, 1948.
20. H. Viervoll and O. Ögrim, Acta Cryst. **2**, 277 (1949).
21. R.W.G. Wyckoff, Crystal Structures, volume I, section e, Interscience Publ. Inc., New York, 1948.
22. W.O. Milligan, H.A. Levy and S.W. Peterson, Phys. Rev. **83**, 226 (1951).
23. R. Mecke and W. Baumann, Physik. Z. **33**, 833 (1932).
24. S.W. Peterson and H.A. Levy, Acta Cryst. **10**, 70 (1957).
25. H. Mendel, Discussions Faraday Soc. **24**, 235 (1957).
26. G.E. Bacon, Neutron Diffraction, Oxford, 1955.
27. L.E. Orgel, Revs. Modern Phys. **31**, 100 (1959).
28. E.R. Lippincott and R. Schroeder, J.Chem.Phys. **23**, 1099 (1955).
29. J.A. Pople, Proc. Roy. Soc. (London), **A 205**, 163 (1951).
30. L. Pauling in "Hydrogen Bonding" (edited by D. Hadži and H.W.Thompson), Pergamon Press, London, 1959.
31. J.O'M. Bockris, Quart. Revs. (London) **3**, 173 (1949).

32. E.J.W. Verwey, Rec. trav. chim. **61**, 127 (1942).
33. H.A. Lorentz, Theory of electrons, Leipzig, 1909.
34. K. Fajans, Z. Elektrochem. **34**, 502 (1928).
35. L. Onsager, J.Am.Chem.Soc. **58**, 1486 (1936).
36. C.J.F. Böttcher, Physica **9**, 937 and 945 (1942).
37. C.J.F. Böttcher, Rec. trav. chim. **62**, 325 (1943).
38. C.J.F. Böttcher, Rec. trav. chim. **62**, 503 (1943).
39. C.J.F. Böttcher, Rec. trav. chim. **65**, 19 (1946).
40. Th.G. Scholte, Thesis, Leiden, 1950.
41. H.W. Joustra, Thesis, Leiden, 1959.
42. K. Lonsdale, Proc. Roy.Soc. (London) **A 247**, 424 (1958).
43. C.J.F. Böttcher, Rec. trav. chim. **65**, 14 (1946).
44. J.S. Rosen, J.Opt.Soc.Am. **37**, 932 (1947).
45. N.E. Dorsey, Properties of Ordinary Water-Substance, Reinhold Publ. Comp., New York, 1940.
46. J.P. Mathieu and Mackenzie Lounsbury, Discussions Faraday Soc. **9**, 156 (1950).
47. L. Pauling, The Nature of the Chemical Bond, Cornell University Press, 1945.
48. A.N. Campbell and E.M. Kartzmark, Can. J.Chem. **33**, 887 (1955).
49. L.G. Sillén, Acta Chem.Scand. **3**, 539 (1949).
50. C.L. van Panthaleon van Eck, H.B.M. Wolters and W.J.M. Jaspers, Rec. trav. chim. **75**, 802 (1956).
51. K.H. Stern and E.S. Amis, Chem. Revs. **59**, 1 (1959).

ACKNOWLEDGEMENT

I wish to express my gratitude to Dr Ir E.L. Mackor for his interest in the work and for the stimulating discussions, and also to Dr H. Mendel for his valuable advice concerning the chapters I and II.

I am very much indebted to the Management of the Koninklijke/Shell-Laboratorium, Amsterdam, for having given me the opportunity to perform this work and for the permission to publish the results of the X-ray diffraction measurements as part of this thesis.

S T E L L I N G E N

1

Bij de berekening van de polariseerbaarheden en de stralen van ionen uit optische refractiemetingen aan oplossingen van electrolyten in water verdient het aanbeveling de waarde 1.50 Å voor de straal van het watermolecule te gebruiken.

Dit proefschrift, Hoofdstuk III.

2

Het is niet te verwachten dat de door Higuchi afgeleide formule voor de berekening van de diëlectrische constante van dispersies uit de diëlectrische constanten van de componenten betere resultaten zal geven dan de door Böttcher afgeleide formule.

W.I. Higuchi, J. Phys. Chem. 62, 649 (1958).
C.J.F. Böttcher, Theory of Electric Polarisation, Chapter XI.

3

De resultaten van de door Tourky en Rizk uitgevoerde metingen ter bepaling van het dipoolmoment van het $SnCl_4$-molecule rechtvaardigen niet hun conclusie dat dit molecule een pyramidale structuur heeft.

A.R. Tourky en H.A. Rizk, J. Phys. Chem. 61, 231 (1957).

4

Het door Blackadder en Hinshelwood voorgestelde reactiemechanisme voor de oxydatie van hydrazobenzeen in alkalisch milieu is op grond van de door hen gegeven experimentele resultaten niet aanvaardbaar.

D.A. Blackadder en C. Hinshelwood, J. Chem. Soc. 1957, 2898.

5

De interpretatie die Mitra en Atreyi geven aan de electrometrische titratiecurve van ureum-formaldehydehars is aan bedenkingen onderhevig.

R.P. Mitra en M. Atreyi, Naturwissenschaften 45, 286 (1958).

De conclusie van Hall dat geluidsrelaxatie tengevolge van het "stoelbed" evenwicht in methylcyclohexaan bij lage frequenties (< 100 KHz) optreedt is onjuist; relaxatie tengevolge van dit evenwicht moet juist bij zeer hoge frequenties (> 100 MHz) worden gezocht.

D.N. Hall, Trans. Faraday Soc. **55**, 1319 (1959).

7

McCusker en Ostdick hebben niet aannemelijk gemaakt dat bij de eerste stap in de reactie tussen BCl_3 en een hexa-alkylcyclotrisiloxaan drie moleculen BCl_3 betrokken zijn.

P.A. McCusker en T. Ostdick, J.Am. Chem. Soc. **80**, 1103 (1958).

8

Het is niet noodzakelijk dat de bromering van tropon tot 2,7-dibroomtropon via het door Nozoe et al. voorgestelde tussenprodukt verloopt.

P.L. Pauson, Chem. Revs. **55**, 41 (1955).
T. Nozoe, T. Mukai, K. Takase en T. Nagase, Proc. Japan Acad. **28**, 477 (1952).

9

Het is niet zonder meer in te zien dat de verklaring, die Carrington, Dravnieks en Symons geven voor de verandering met de tijd van het electronenspinresonantiespectrum van het mono-negatieve ion van anthraceen juist is.

A. Carrington, F. Dravnieks en M.C.R. Symons, J. Chem. Soc. **1959**, 947.

10

Het is ongewenst om de "spin-only" waarde van het magnetisch moment op te geven als $n\mu_B$, waarin n het aantal ongepaarde electronen en μ_B het Bohr-magneton is.

W.L. Roth, Phys. Rev. **110**, 1333 (1958).
J.B. Goodenough, D.G. Wickham en W.J. Croft, J. Phys. Chem. Solids **5**, 107 (1958).

J. Heemskerk, 17 december 1959.

Op verzoek van de Faculteit der Wis- en Natuurkunde volgt hier een kort overzicht van mijn academische studie.

In 1948 behaalde ik het einddiploma H.B.S.-B aan de Dalton H.B.S. te 's-Gravenhage en begon ik mijn studie aan de Rijksuniversiteit te Leiden, waar ik in mei 1952 het candidaatsexamen Wis- en Natuurkunde, letter f, aflegde. De studie werd voortgezet onder leiding van de Hoogleraren Dr C.J.F. Böttcher, Dr L.J. Oosterhoff en Dr E. Havinga. In mei 1955 legde ik het doctoraalexamen af (fysische chemie met theoretische organische chemie en organische chemie). Van oktober 1952 tot augustus 1955 was ik assistent bij de afdeling fysische chemie II te Leiden.

Na vervulling van de militaire dienstplicht trad ik in oktober 1956 in dienst van het Koninklijke/Shell-Laboratorium, Amsterdam. De Directie van dit laboratorium stelde mij in de gelegenheid om gedurende een jaar werkzaam te zijn aan het laboratorium voor fysische chemie van de Universiteit van Oxford. Het aldaar verrichte onderzoek stond onder supervisie van Mr. R.P. Bell, F.R.S. Daarna was ik nog enige tijd, onder leiding van Prof. Dr C.J.F. Böttcher, werkzaam aan het laboratorium voor fysische chemie der Rijksuniversiteit te Leiden. Het in dit proefschrift beschreven onderzoek werd gedeeltelijk aldaar en gedeeltelijk in het Koninklijke/Shell-Laboratorium, Amsterdam, verricht.